This dissertation has been
microfilmed exactly as received

67-9491

MILACEK, Leonard, 1935-

PROTON RADIATION INDUCED BLISTERING OF ALUMINUM.

The University of Oklahoma, Ph.D., 1967
Engineering, metallurgy

University Microfilms, Inc., Ann Arbor, Michigan

Downloaded from SHAREOK. Persistent Handle URL: https://hdl.handle.net/11244/2159

THE UNIVERSITY OF OKLAHOMA

GRADUATE COLLEGE

PROTON RADIATION INDUCED BLISTERING OF ALUMINUM

A DISSERTATION

SUBMITTED TO THE GRADUATE FACULTY

in partial fulfillment of the requirements for the

degree of

DOCTOR OF PHILOSOPHY

BY

LEONARD MILACEK

Norman, Oklahoma

1967

PROTON RADIATION INDUCED BLISTERING OF ALUMINUM

APPROVED BY

Raymond D. Daniels

Charles J. Martin

R. J. Block

R. Craig Turner

ABSTRACT

Investigation of the effects of low energy proton irradiation of aluminum and gold samples demonstrated that protons in the energy range 7 to 450 Kev could cause permanent damage to the materials. This damage is in the form of pitting and blistering of the metal surface. These observations are of significance to the application of these materials for thermal control surfaces in space flight applications.

High purity aluminum exhibited surface pitting and blistering in the irradiated area. Pitting occurred during irradiation and is the predominant surface damage at lower proton energies. Blistering occurs spontaneously at room temperature for samples irradiated at energies of 70 Kev or lower. Samples irradiated at energies of 100 Kev or higher may exhibit a small amount of spontaneous blistering, but annealing above 200°C. is necessary to produce large concentrations of blisters.

The proton radiation induced pitting and blistering phenomena have been studied using optical and electron microscopy. Attention was given to determine the influence of crystal orientation, surface preparation, material purity, substructure, and cold work on the manner of occurrence and appearance of blistering. These observations were correlated with radiation and environmental parameters to delineate the processes responsible for pitting and blistering.

Blistering is attributed to the trapping of protons and their agglomeration as hydrogen within voids in the lattice near the metal surface. Hydrogen pressure within these voids causes an expansion which is observed as blisters on the metal surface. Pitting was shown to be associated with exfoliation of the oxide on aluminum, and pits could be removed by oxide stripping. Pitting is explained by agglomeration of hydrogen at the oxide-metal interface with subsequent rupture and exfoliation of the oxide.

The dependence of the effects observed upon metal purity and microstructure are consistent with the model for hydrogen agglomeration proposed. Definite correlations of pitting and blistering with crystal orientation were also demonstrated. The theoretical implications of these results are discussed.

ACKNOWLEDGMENTS

The author wishes to express his gratitude to those whose assistance made the completion of this work possible.

In particular, appreciation is extended to Dr. R. D. Daniels, Professor and Associate Dean, College of Engineering, under whose guidance and council this program was performed.

I wish to thank Messrs. Jim Thompson and Robert Skinner for their help with some of the experimental work reported herein.

The author wishes to thank Messrs. Michael Gamble, Jim Cooley, and Bill Holland of the AVCO Corporation/Tulsa Division, who performed the irradiations and assisted in the guidance and council of this program.

Finally, thanks are to be extended to National Aeronautics and Space Administration for their financial support for the author and the research funds for this program.

TABLE OF CONTENTS

Page

LIST OF FIGURES v

Chapter

I. INTRODUCTION 1

Statement of the Problem 5

II. REVIEW OF THE LITERATURE 12

III. DESCRIPTION OF EXPERIMENTAL MATERIAL, APPARATUS AND PROCEDURE 18

Specimen Preparation 18
Specimen Irradiation 21
Specimen Examination 21

IV. RESULTS 23

V. DISCUSSION OF RESULTS 55

VI. CONCLUSIONS 74

APPENDIX A 77

APPENDIX B 81

LIST OF REFERENCES 84

LIST OF FIGURES

Figure		Page
1.	Fractured Blisters on 6061 Aluminum Alloy.	6
2.	Irradiated Band on 6061 Aluminum Alloy.	7
3.	Blistered Surface from which Oxide Has Been Chemically Removed	9
4.	Large Blisters which Show Elongation along Cold Work Striations	10
5.	Irradiated Polycrystalline Specimen with Oblique Illumination	25
6.	Pitting of Oxide on Polycrystalline Specimen	26
7.	Irradiated Polycrystalline Specimen with Oxide Chemically Removed	27
8.	Irradiated and Annealed Polycrystalline Specimen with Oxide Chemically Removed.	28
9.	Edge of Irradiated Area of Pitted and Blistered Specimen	30
10.	Oxide Removal from Irradiated Area	31
11.	Partial Oxide Removal from Irradiated Area	32
12.	Identification Classification and Orientation of Grains within Irradiated Region. Classification is Based upon Degree of Pitting	35
13.	Orientation of Grains Based upon Classification According to Degree of Pitting	36
14.	Identification Classification and Orientation of Grains within Irradiated Region. Classification is based upon Degree of Blistering.	37
15.	Orientation of Grains Based upon Classification According to Degree of Blistering.	38
16.	Composite Diagram Showing Orientations of Light, Medium, and Heavy Pitting Represented as Areas on Stereographic Triangle	39

Figure Page

17. Composite Diagram Showing Orientations of Light, Medium, and Heavy Blistering Represented as Areas on Stereographic Triangle. 40

18. Blisters along Hexagonal Structure Associated with Impurity Segregation 41

19. Delineation of Impurity Segregation Structure by Excessive Electropolishing 43

20. Pitting along Substructure in Recrystallized Aluminum. . . 44

21. Structure in the Oxide due to Electropolishing 46

22. Elongated Blisters; Some of which have Collapsed. Heavy Blister Concentration along Grain Boundary 47

23. Limited Degree of Pitting and Blistering Along Grain Boundaries 48

24. Large Blisters Situated along Scratches. 50

25. Diffuse Scattering of Light Associated with Blisters in Irradiated Area 53

26. Blisters on Gold 54

27. Annotated Illustration of Irradiation and Blistering Process. 57

28. Annealed Specimen with Oxide Chemically Removed. 58

29. Elongated Blisters; Some of which have Collapsed 63

30. Pitting and Blistering with Concentration Variation Between Two Grains 64

31. Blisters at Edge of Irradiated Area. 65

32. Blistering Due to Void Formation at Oxide-Metal Interface. 67

BLISTERING OF METALS BY PROTON IRRADIATION

CHAPTER I

INTRODUCTION

The advent of spaceflight in the presence of solar winds and Van Allen radiation belts has presented the question of what effects such an environment may introduce into materials utilized in space. The major part of this space radiation is composed of low energy protons which originate from cosmic rays and solar winds. Proton energies associated with solar winds are in the range of 1 to 9 Kev while secondary protons associated with cosmic rays are concentrated at the energy levels of 1 Mev or less (1). Secondary protons are produced by high energy cosmic rays reacting with oxygen and nitrogen nuclei in the Earth's upper atmosphere.

Research on the effects of charged particle irradiation on materials has been primarily concerned with high energies ($>$1 Mev) associated with nuclear reactions and high energy accelerators. The effects of such high energy charged particle radiation are of a different nature than expected with lower energy particles. High energy particles penetrate deeper into the material and produce a greater amount of structural damage within the material. In contrast, the low penetration depths associated with low energy ions can be expected to

produce surface effects which are not observed on materials irradiated with high energy particles.

Limited amount of research has been conducted with very low energy charged particle irradiation in connection with vacuum and gas filled electronic tubes (2). The primary form of damage encountered here has been sputtering, the removal of atoms or molecules from a target material by ion bombardment. Although the principles discovered from these studies may prove useful, the materials studied in this research have been primarily oxide free surfaces. The results obtained from these studies are not expected to be fully applicable to oxide covered spacecraft materials.

Low energy proton irradiation effects upon thermal control surfaces have been investigated by Anderson and Dahms, and Gillette et al (3,4). The surfaces studied consisted of metal films vapor deposited upon a variety of substrate materials and some paint coatings. The damage to these surfaces has been evaluated by determining the degree of change in solar absorptance. The physical damage to the surfaces has been reported to be due to sputtering and gas void formation at the metal film-substrate interface.

Although low energy proton irradiation produces other degradation effects in metals, the most obvious effects are introduction of hydrogen gas into the metal lattice and surface sputtering of the metal. While hydrogen is capable of embrittling many common bcc and hcp metals, its detrimental effects in fcc aluminum are restricted to void and blister formation. Blistering and internal void formation in aluminum and its alloys caused by the presence of hydrogen plagued

the metal industry for many years before the specific problem of hydrogen pickup through proton irradiation in outer space environments was even envisioned. The problem of blistering and internal void formation is commonly observed in aluminum castings and arises from exposing molten aluminum to hydrogen containing atmospheres. The hydrogen containing voids form upon solidification of the molten aluminum. The relatively high solubility of hydrogen in molten aluminum contrasted by its low solubility in solid aluminum produces a rejection of excess hydrogen from the metal lattice. This excess hydrogen, with proper time and temperature, agglomerates to form voids. These voids may be near enough to the free surface to cause a swelling or blistering of the metal surface. Although improvement of industrial practices has overcome many of the difficulties associated with hydrogen in aluminum alloys, there is a continuing interest in the subject because of the potential for hydrogen pickup in the various phases of fabrication of aluminum and because a detailed knowledge of the processes involved is still lacking.

Nuclear fission with the production of fission products has been observed to cause gas containing voids in materials. These fission product atoms may exist within the lattice in the form of solid, liquid, or gas depending upon the temperature of the materials. It has been calculated that one inert gas atom is formed for every four atoms fissioned (5). Although inert gas atoms are not normally soluble in metals, the gas atoms formed during the fission process are randomly distributed throughout the lattice and may be considered to be in an abnormal state of solution. Since the greater portion of the inert gas atoms formed are xenon and krypton whose diffusion rates are significant

only near the melting point of the materials, the movement of these inert gas atoms at moderate temperatures is limited to void formation within the materials. These voids are capable of movement by a surface self-diffusion mechanism, but very little evolution of the gas occurs at the surface of the materials (6,7). Such formation of inert gas filled voids in the material produces an internal pressure which is capable of swelling the material (8-10). This pressure can be of sufficient magnitude to introduce local stresses greater than the yield stress of the material. Ductile materials are capable of accommodating this stress by swelling, but a brittle material might be expected to rupture from a pressure buildup.

Although the phenomenon of surface sputtering has long been known, its degradation effects have not been studied as extensively as gas void formation. Only in recent years, with the increased research in space, plasma, vacuum, surface and solid state physics, has sputtering received appreciable attention. Sputtering has been viewed either as a useful phenomenon, an interesting phenomenon, or simply as a nuisance. It has been useful in thin film deposition and in the cleaning and etching of material surfaces; it has been interesting from the viewpoint of the solid state physicists; and it has been a nuisance for its damaging effects to material surfaces. It is in this area of its damaging effects on materials where the most recent research activities have been directed.

Projected utilization of materials for prolonged periods in low energy particle-containing space environments has necessitated serious consideration of this factor in spacecraft design. While such

factors might reasonably have been neglected in past satellite designs where the useful life expectancy of the vehicle was short term, future crafts will be expected to operate for longer durations even in the presence of such radiation. If the characteristic effects of low energy proton irradiation on materials can be determined and if the fundamental processes involved can be ascertained, such knowledge can be utilized in space vehicle design. In addition, information obtained from such a study may contribute to our knowledge of the more basic problem of gases in metal.

Statement of the Problem

During the early stages of development of the AVCO/Tulsa space environment simulation facility, work began on the ion-metal film phenomenon. The ion-metal film phenomenon appeared as discolorations on metal surfaces which had been irradiated by a proton beam. The discolorations appeared upon some anodized aluminum alloy (6061-T6) samples in the as-irradiated condition while on other samples of the same material it appeared only after subsequent annealing. Microscopic examination at low magnification revealed a rough texture on the irradiated portions of otherwise polished surfaces, and examination at higher magnifications revealed that the surface roughening was due to a blister-like eruption on the surface of the aluminum.

Additional experiments, utilizing unanodized mechanically polished aluminum alloy (6061-T6) and high purity aluminum samples, showed the reproducibility of this blister phenomenon. Figures 1 and 2 are macro and photomicrographs of a piece of aluminum alloy sheet which was irradiated with 200 Kev protons to an integrated flux of 10^{17}

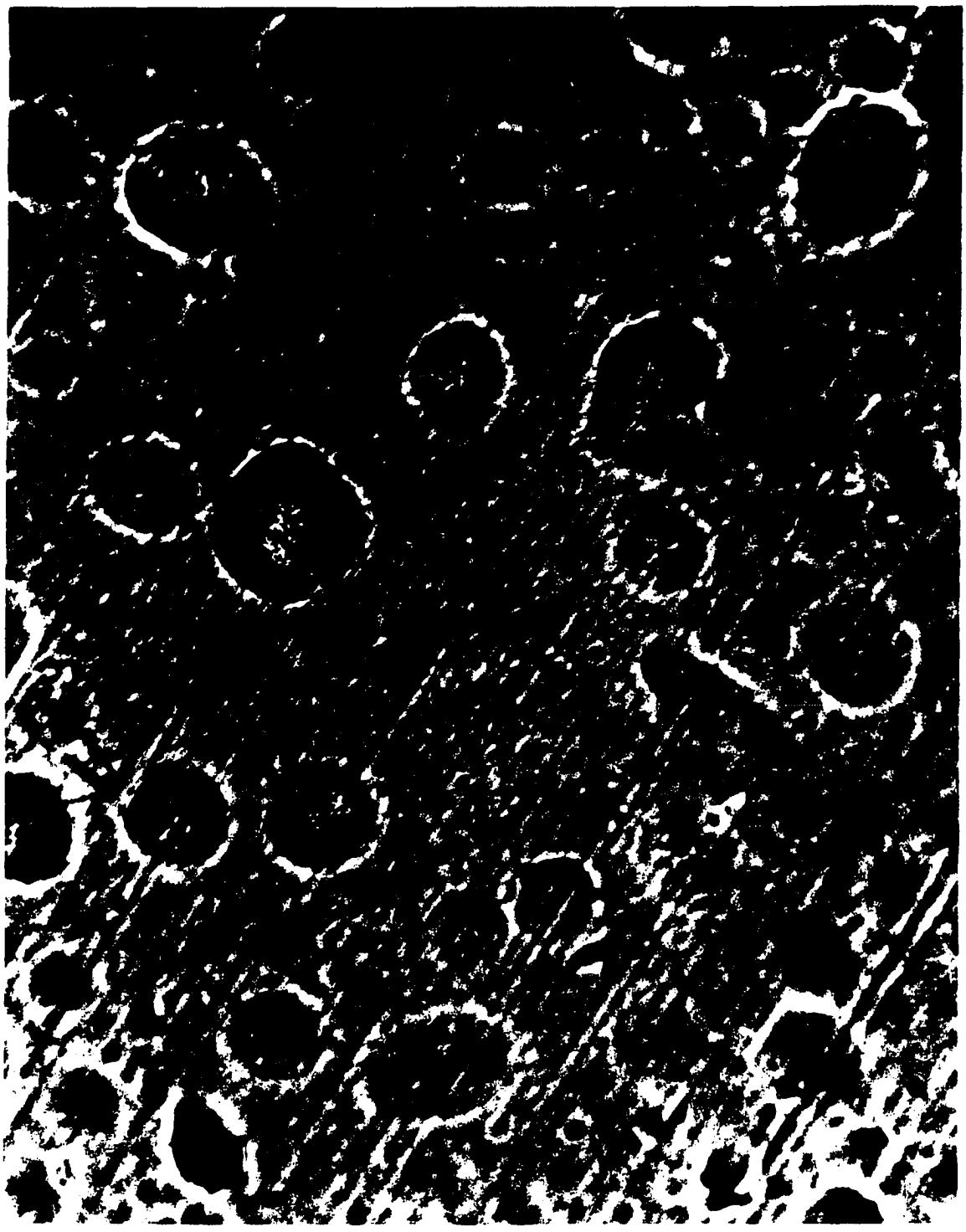

Figure 1. Magnification 165X. Bright Field Illumination. 6061 Aluminum Alloy Annealed. 200 Kev Protons. Fractured Blisters on 6061 Aluminum Alloy.

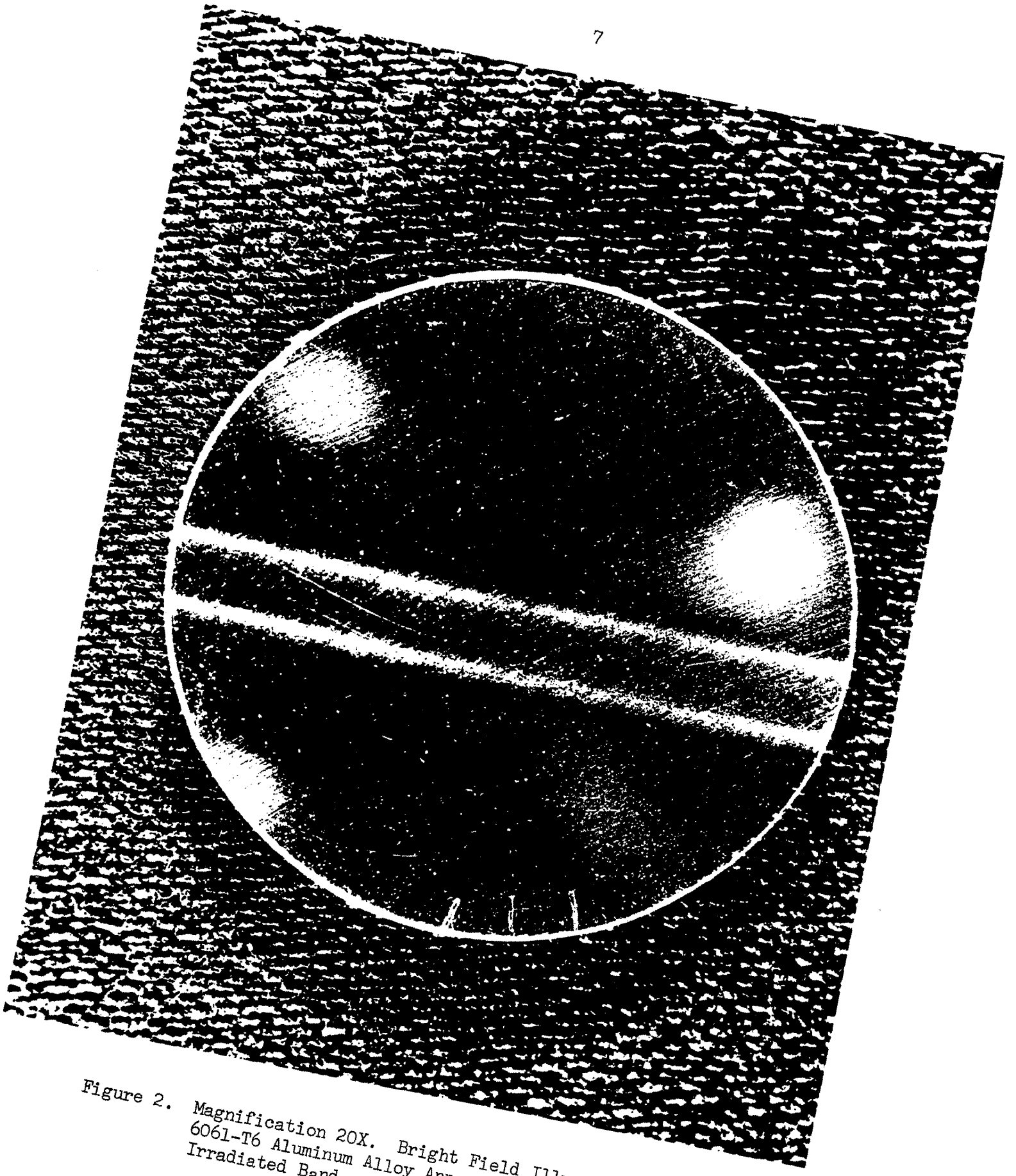

Figure 2. Magnification 20X. Bright Field Illumination. 6061-T6 Aluminum Alloy Annealed. 200 Kev Protons. Irradiated Band on 6061 Aluminum Alloy.

protons/cm^2 and then annealed for 10 minutes at 300°C. Figure 3 is a photomicrograph of a high purity aluminum sample irradiated with 100 Kev protons to an integrated flux of 10^{17} protons/cm^2 and annealed for 10 minutes at 300°C.

Visual examination revealed that the low energy proton irradiation causes a significant change in the reflectance characteristics of metallic surfaces subjected to such bombardment. The obvious damage is surface blistering with additional damage on the high purity aluminum in the form of pitting or cratering of the surface. Comparison of a high purity aluminum specimen with an alloy aluminum specimen (Figures 3 and 4) also reveals an apparent dependence of blister size and geometry upon impurity content and rolling effects in aluminum.

These observations of blistering and pitting upon aluminum introduced the questions of what are the mechanisms of the processes responsible and what are the material and environment parameters of significance in these processes. The objectives of the present work are to determine: (1) the conditions under which proton irradiation of aluminum will produce surface blistering and pitting, (2) the dependence of the phenomena on material structure, and (3) the effects of various sample preparation procedures. The basic parameters considered in the blistering and pitting process are: (1) the penetration depth and distribution of protons in aluminum, (2) the solubility of hydrogen in aluminum, (3) the mobility of hydrogen in aluminum, and (4) the effects of lattice defects, impurities,and the oxide surface film on the distribution and transport of hydrogen in aluminum. Theoretical questions involved are: (1) the mechanisms of transport and evolution of hydrogen in the metal, (2) the roles of

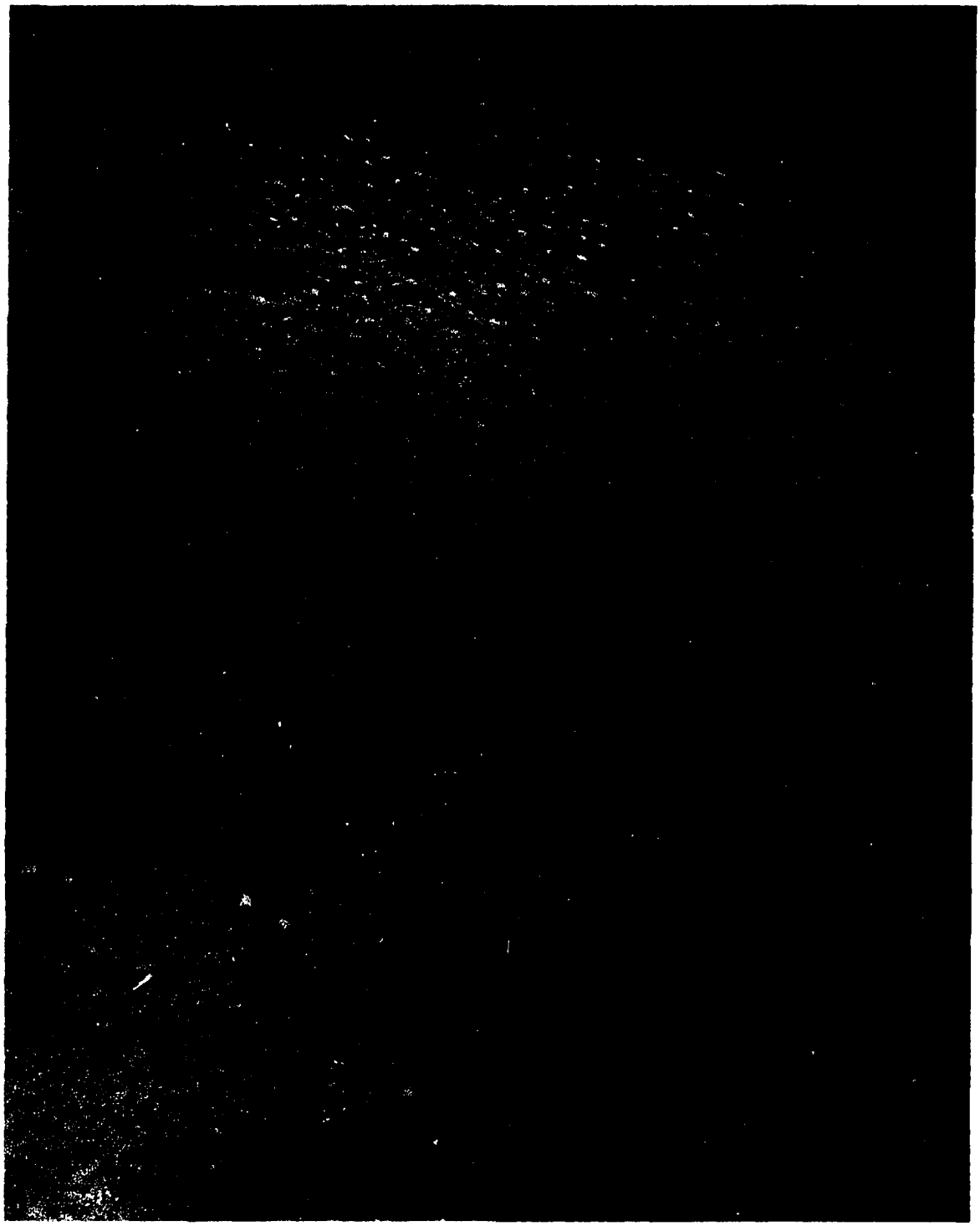

Figure 3. Magnification 1500X. Enlarged 1.8X. Numerical Aperature 1.4. Bright Field Illumination. High Purity Aluminum-Annealed. 100 Kev Protons. Blistered Surface from which Oxide has been Chemically Removed.

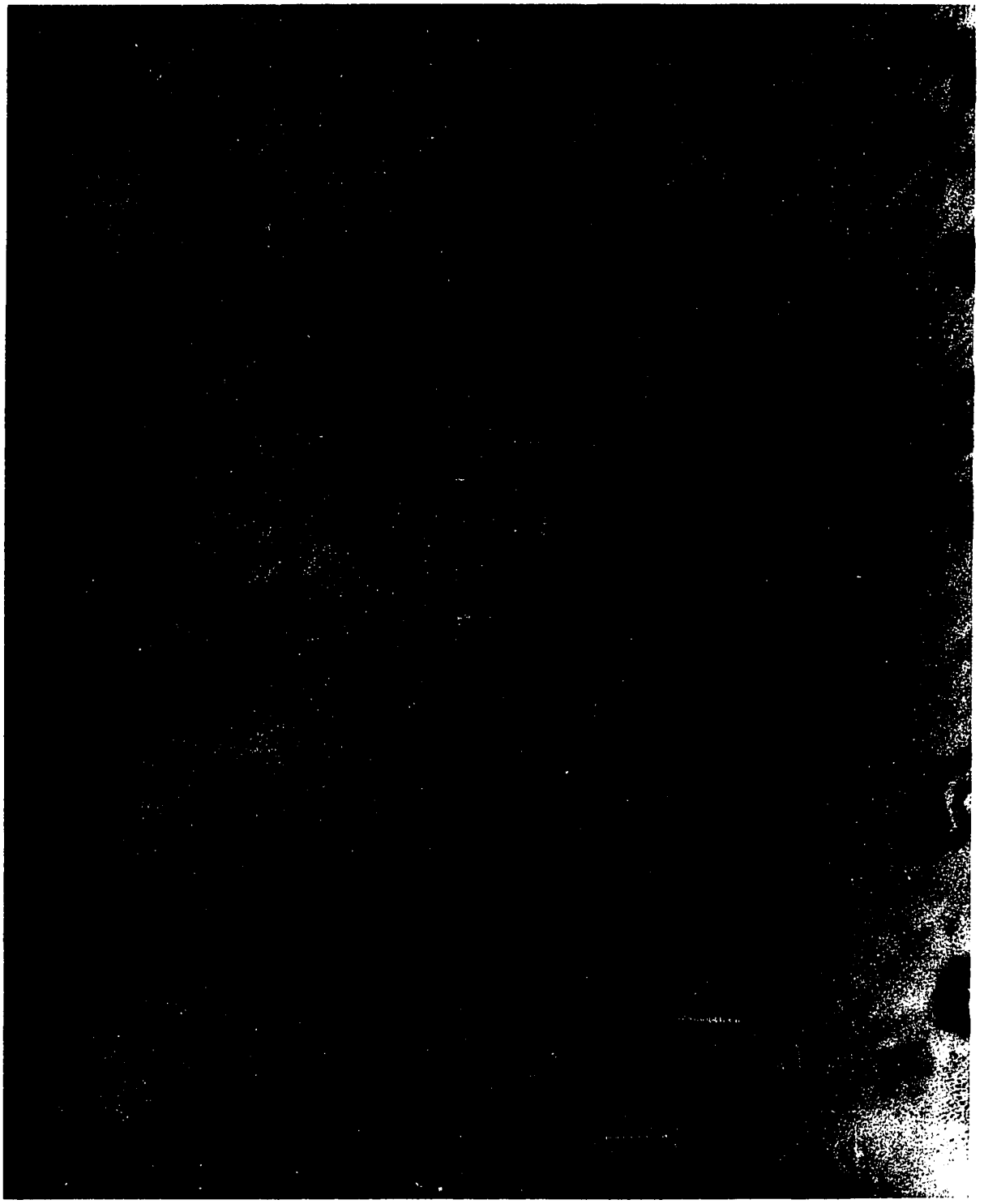

Figure 4. Magnification 320X. Bright Field Illumination. 6061-T6 Annealed. 200 Kev Protons. Large Blisters which Show Elongation Along Cold Work Striations.

lattice defects, impurities and the oxide surface film in the transport and evolution processes, (3) ion-target interaction, and (4) the mechanism of blister formation.

Observation of blisters on high purity aluminum and aluminum alloy specimens introduced the question of what role did the presence of a stable aluminum oxide have in the blistering mechanism. To determine if the presence of an oxide layer was a necessary prerequisite for blistering, gold with its lack of an oxide was chosen as a material for study. Also, to reduce the number of parameters entering into the processes, high purity metals were used exclusively throughout this study.

CHAPTER II

REVIEW OF THE LITERATURE

The effects of proton bombardment of metal surfaces have received appreciable attention only within recent years. The work of Ells and Evans (11), Kaminsky (12), and Pemsler and Rapperport (13) were among the first results published concerning hydrogen agglomeration within a bulk metal where the hydrogen was introduced by ion bombardment. Ells and Evans and Pemsler and Rapperport were concerned with evaluating the effects of 7 Mev protons, which penetrated relatively large distances into the metal and therefore did not cause observable surface damage. The nature of the proton penetration and the hydrogen behavior determined in these investigations is useful as a guide to analysis and interpretation of the surface blistering phenomenon observed at lower proton energies.

Ells and Evans examined the agglomeration of hydrogen in 7 Mev proton irradiated samples ranging from very high purity aluminum to Al-Mg alloys. The specimens were cross-sectioned perpendicular to the hydrogen containing layer in such a manner that its distance from the edge could be determined. Optical microscope examination revealed the high energy proton penetrated into the aluminum a distance of approximately 0.033 cm. and formed a hydrogen containing layer 0.004 cm. thick.

Hydrogen concentrations in this layer were calculated to be from .16 to 22 ppm. Ells and Evans reported that practically all samples irradiated at temperatures of 300°F. or less exhibited fine agglomerates (pockets of hydrogen) in the as-irradiated condition. Intragranular agglomerates appeared as pits with radii of from 0.5 micron to about 5 micron, while agglomerates in the grain boundaries were observed as cracks up to and in excess of 10 microns in width. These grain boundary agglomerates appeared at distances up to 0.02 cm. from the main hydrogen-containing layer with this effect being particularly pronounced in the high purity aluminum. Heating for one hour at 300°C. produced a general coarsening of the agglomerate size in the main hydrogen-containing layer and a considerable enlarging of agglomerates at grain boundaries intersecting the layer. In addition, there was a dispersal of some agglomerates both at the edges of the layer and also in grain boundaries at locations outside the main layer. Heating for one hour at 500°C. produced an additional increase in agglomerates which disappeared with further heating. Examination of specimens irradiated at temperatures about 300°C. revealed no evidence of a hydrogen-containing layer in the as-irradiated condition or after annealing.

Ells and Evans also studied the effects of prior history of the material upon the agglomeration of hydrogen and report that materials irradiated in the cold worked condition were similar to those irradiated in the annealed condition. The addition of up to 3 weight per cent magnesium, had a slight tendency to decrease the number of agglomerates formed. The general behavior of this alloy was similar to the ultra pure aluminum.

Pemsler and Rapperport in their work with proton bombarded beryllium found results similar to those reported by Ells and Evans. The only major difference being a lack of hydrogen agglomeration in beryllium in the as-irradiated condition even though a hydrogen layer concentration of 80 ppm was achieved. This may be explained by the lower diffusion coefficient for hydrogen in beryllium which restricts necessary movement for the agglomeration of hydrogen.

Kaminsky bombarded single crystals of silver and copper with 0.1 to 4 Mev protons, deutrons, and helium ions. Gas bubbles were observed on the surface, and by use of a mass spectrometer the bubbles were observed to re-emit the incident species as the bubbles exploded. The apparent blister density was correlated with gas bursts.

Recent reports of surface blistering of metals under proton bombardment have been made by Gillette, et al (14) and also by Primak, et al (15). Both of these sources report spontaneous blistering of aluminum upon bombardment by low energy protons. Neither group analyzed the microstructural or surface conditions associated with this effect.

A second deleterious effect of ion bombardment upon metal surfaces is the phenomenon of sputtering. Although low energy ion bombardment of a metal surface is known to remove atoms, it is uncertain whether serious damage to the skin of a spacecraft will result from exposure to space irradiation. The meager knowledge of sputtering yields (number of particles removed per impinging particle) of oxide covered metal surfaces necessitates a survey of the information concerning bare metal sputtering yields to make estimates of results to be

expected with oxide covered aluminum. Two references were found in the literature concerning the sputtering of Al_2O_3 on aluminum (16,17); both report the oxide was attacked noticeably less rapidly than aluminum metal.

The validity of published sputtering data is often difficult to evaluate since only in the more recent work have authors become aware of the many parameters which enter into the phenomena. These parameters involve both the material and the ion-target interactions. Refinements in vacuum systems and precision measuring equipment have also produced a greater consistency among the results of various investigators. These refinements are reflected in lower threshold energies and drastically revised sputtering yields.

G. K. Wehner, et al (18-21) studied the effects of ion bombardment upon the surfaces of various metallic and non-metallic materials. Their work has been primarily concerned with the use of lower energy particles to determine sputtering yields and threshold energies for various ion-material combinations. They have attempted to identify mechanisms of sputtering which are capable of explaining experimental results.

The momentum-transfer theory is today widely accepted as the means of target atom ejection during ion bombardment. This theory assumes that an impinging particle transfers sufficient momentum to surface-bound atoms for the impacted atoms to escape from the surface. Neither the mechanism of transfer nor the energy which the bound atom must acquire is known, but the energy required is thought to be either the energy of sublimation ($\sim$4 ev, depending on the material and on the

location of the atom in the crystal structure) or the displacement energy in radiation damage theory ($\sim$25 ev for most substances). The effects are complicated by such factors as: (1) preferential sputtering which takes place in the direction of close-packed chains in single crystals, (2) sputtering yields which are a function of the angle of incidence of the ions, and (3) ion-target chemical interactions.

Although the influence of proton energy on blister formation must be explained on the basis of particle penetration in the aluminum lattice, data on proton penetration in the low energy ranges are meager. Also, the available penetration data in the literature is not consistent among the various authors. The principal sources of these data are range-energy curves by Young (22) for 1-25 Kev protons in aluminum, energy loss versus proton energy for 50-400 Kev protons in aluminum by Warshaw (23), and range-energy curves for 0-350 Kev protons in aluminum and gold by Wilcox (24). These reported results indicate an expected penetration in aluminum of approximately 0.1 to 1.5 microns for protons in the 10 to 200 Kev range. The energy losses suffered by 4 to 30 Kev protons in passing through aluminum oxide are reported by Wijngaarden and Duckworth (25).

Recent calculations of the ranges of penetration of energetic ions into crystalline solids based upon a theoretical model show these ranges to be strongly dependent upon crystal orientation (26). The model used in these calculations assumes that the moving atoms lose all their energy through binary eleastic collisions with the atoms of the solid. The interaction potential assumed was an exponentially screened Coulomb (Bohr) potential. The authors found that neither the hard

sphere approximation nor the inverse r-squared approximation to the Bohr potential is particularly good. The orientation dependence of the depth of penetration is explained as a consequence of the tendency of the lattice to focus moving particles into channels bordered by relatively closely packed atomic rows. These calculations predict penetration ranges greater than normal in the directions of low indices. The order of ion penetration ranges in the face centered cubic lattice is [011]>[001]>[111]. Recent experimental evidence by Piercy, et al (27) utilizing 40 Kev $^{85}Kr^{+}$ ions impinging upon aluminum has substantiated these calculations.

The solubility of hydrogen in solid aluminum has been determined by various authors, but the results of Ransley and Neufeld (28) are the most widely accepted values. The solubility for hydrogen in annealed aluminum increases with temperature with the maximum of 0.036 $cm^3/100g$ (0.032 ppm.) occurring at the melting point (660°C.). This value represents the solubility of aluminum under laboratory conditions, but under industrial conditions aluminum is believed to be capable of dissolving greater quantities of hydrogen due to the presence of water vapor (29-30). Also, determinations of hydrogen in deformed and cast metals have produced solubilities up to 160 $cm^3/100g$ for deformed material and 70 to hundreds of $cm^3/100g$ for cast materials, respectively (31).

The solubility of hydrogen in gold is not well known. Early authors reported hydrogen to be insoluble in gold (32-33), but more recently authors (34) report a limited solubility of 0.045 $cm^3/100g$ at 700°C. and 0.09 $cm^3/100$ g at 900°C.

CHAPTER III

DESCRIPTION OF EXPERIMENTAL MATERIAL, APPARATUS, AND PROCEDURE

The high purity aluminum ingots were obtained from Reynolds Aluminum Company. Spectroscopic analysis of the material performed by Reynolds Research Laboratories indicated the major impurities to be iron 0.001% and magnesium 0.001%. All other possible impurities were below the limit of reliable analysis. The high purity gold was obtained from United Mineral and Chemical Corporation. The purity was 99.999% with no analysis given of the impurities.

The experimental procedures used in this study may be divided into three categories: (1) specimen preparation, (2) specimen irradiation, and (3) specimen examination.

Specimen Preparation

The high purity aluminum was fabricated into specimens for irradiation by one of two procedures: (1) crystal growth from the melt, or (2) swaging and annealing. To produce single crystals, elongated pieces were cut from the ingots, swaged into long cylinders, and remelted in a cylindrical graphite crucible under an argon atmosphere. The crucible was mounted in a vertical Vycor tube and solidification of the aluminum was controlled by traversing the hot zone of a tube furnace surrounding the sample (Modified Bridgeman technique). Conditions for

unidirectional solidification were obtained under appropriate traverse conditions (growth rates were at 4 to 8 cm per hour). This technique was used to prepare single crystal rods of 3/8 inch diameter by about 9 inches long. Samples for irradiation, which were 3/8 inch diameter by 1/2 inch long, were cut from rods prepared in this manner. This sample size was initially dictated by the dimensions of the sample holder in the hot stage microscope and for convenience in polishing the surface to be irradiated.

Large-grain polycrystalline aluminum specimens were obtained by recrystallization and extended anneal at 650°C. of ingot material which had been swaged into 3/8 inch diameter rods. The grain size was controlled by the amount of grain growth allowed to occur when the specimens were held at the recrystallization temperature. Large grain samples prepared in this manner were used to study the effects of crystallographic orientation of the surface on the tendency for pits and blister formation under proton bombardment. A variation of this technique was developed when a study of orientations in the swaged and recrystallized material revealed a preferred orientation with an exclusion of orientations near the (110) pole. Several sample rods were swaged to a diameter slightly larger than 3/8 inch and then pulled in tension until the diameter was reduced to 3/8 inch. It was found that recrystallization of aluminum elongated in tension in this manner produced (110) orientations.

Specimens of the aluminum, 6061-T6, were prepared by blanking out discs of appropriate size from rolled sheet.

Specimens of high purity gold in the form of polycrystals were produced by a long time grain growth anneal.

The surface preparation of the high purity aluminum consisted of a mechanical polish on wet abrasive laps using 0.3 micron alumina and an electropolish in a 2:1 methyl alcohol-nitric acid solution (35). The electropolishing solution was cooled in an ice water bath, the current density was 1 amp/cm^2, the cathode was stainless steel, and a wax covered aluminum alloy clip served as a specimen holder. The anode was intermittently agitated during the duration of the 2 to 4 minute polishing period. The specimens were rinsed in distilled water followed by a methyl alcohol rinse and dryed in an air stream.

The surface preparation of the 6061-T6 aluminum alloy was limited to a mechanical polish on wet abrasive laps using 0.3 micron alumina.

The surface preparation of the gold specimens was a mechanical polish on wet abrasive laps using a 0.3 micron alumina followed by an electropolish in a solution consisting of 75 g KCN, 16g $KNaC_4H_4O_6$, 10g $K_4Fe(CN)_6$, 16g HPO_3 (Solid), 4g CuCN, 3.5ml NH_4OH, and 1000 ml of water (35). A stainless steel cathode was used with the solution at 60°C. and a current density of 1 amp/cm^2. The specimen holder was of stainless steel wire. The anode was agitated rapidly in the electrolyte during operation.

Observations of what appeared to be oxide removal and apparent lack of blistering on some samples irradiated with 30-50 Kev protons prompted a study of the oxide thickness on 99.997% aluminum. (The technique utilized for this study is presented in Appendix A). The

oxide barrier layer on electropolished aluminum surfaces was found to be approximately 9 Å while the porous layer was approximately 50 Å. These values are within the ranges of oxide thicknesses on high purity aluminum reported in the literature.

Specimen Irradiation

A Van de Graaff accelerator was used to irradiate samples with protons. The accelerator was equipped with an analyzing magnet system for mass analysis of the ion beam. The target chamber operates in a range from 5×10^{-9} to 3×10^{-10} mm of Hg. The target holders used in this work were provided with the capability of cooling or heating the specimen by passing fluids at the desired temperatures through the holders. These irradiations were performed by the AVCO Corporation in facilities at the AVCO Instrument Division, Tulsa, Oklahoma.

Specimen Examination

The examination of irradiated specimens was performed primarily with the optical microscope, with an electron microscope being utilized in some of the later studies. Specimens were examined on the optical microscope under normal bright field, low angle oblique, high angle oblique, and dark field illumination. Under low angle oblique illumination, the illuminating source is adjusted a few degrees from the normal to the specimen surface. Under high angle oblique illumination the light path from the source to the specimen is external to the lens system and at an angle of 30-45 degrees from the normal to the specimen surface.

A hot-stage microscope assembly was used in the early stages of this research. The unit consists of a Unitron Model BU-11 metallograph with a HHS heating stage and associated vacuum pumping and power control console. This unit was utilized with aluminum specimens heated under a vacuum of 2×10^{-5}mm of Hg up to temperatures of 500°C. Temperature was manually controlled by a variac. Temperature was measured with a platinum-platinum-13% rhodium thermocouple built into the vacuum heating stage and connected to a direct reading pyrometer.

Electron microscope examination of the specimens was conducted on a RCA EMU-2. A single stage formvar replication technique was utilized. Gold shadowing was used with the angle of shadowing dictated by structure in the replica. A low angle of 5-10° was used to delineate fine detail while a larger angle of 10-20° was used to delineate the gross features.

CHAPTER IV

RESULTS

The experimental approach used in this investigation centered on determining the effects of irradiation parameters and properties of the metal upon the production of observable surface blistering or other defects. The irradiation parameters which could be controlled were energy, integrated flux, specimen temperature, and identity of the impinging particles. Although these external parameters were considered determining factors, the effects of proton bombardment were found to be sensitive also to certain basic microstructural characteristics of the metal itself and to the techniques utilized in the preparation of the specimens. Attempts were made to control the metal specimen parameters or internal parameters, but some of these factors which exerted a significant effect upon the results obtained were difficult to delineate and detect. Perfection of the techniques utilized in specimen preparation and in the subsequent examination of the irradiated specimen surfaces introduced some degree of uniformity in the results, but control of all microstructural variables was not possible.

Proton irradiation energies of 7 to 450 Kev were used in this study with the majority of the specimens irradiated in the range of 10-200 Kev. The limits on energy were determined by the capabilities

of the Van de Graaff accelerator. The flux rates varied from 1.5 x 10^{12}p/cm^2/sec to 11.8 x 10^{12}p/cm^2/sec with total integrated fluxes of 10^{16}p/cm^2 to 3.5 x 10^{17}p/cm^2. Specimen temperature during irradiation was closely controlled. Specimens were irradiated at several temperatures within the range -196°C. to 200°C. Most samples were irradiated at 15°C.

Blistering and pitting were observed to occur upon high purity aluminum surfaces within limits of the above parameters with the distribution and degree of pitting and blistering influenced by the processing history and crystallographic orientation of the specimen material. As an example of the effects observed, the following series of photographs, Figures 5-8, shows the surface of a high purity aluminum specimen irradiated with 100 Kev protons to an integrated flux of 10^{17} p/cm^2. The pitting and blistering illustrated in these figures are of the normal size and distribution found in this material. Examination of the specimens in the as-irradiated condition at low magnification with high angle oblique illumination revealed diffuse scattering of light from the irradiated portions of the surface (Figure 5). This diffuse scattering was associated with a pitting of the specimen surface. The appearance of the aluminum surface in the as-irradiated condition is shown with normal illumination at high magnification in Figure 6. The pitting of the surface is visible, and the variation in concentration of pits among three separate grains is evident. Figure 7 shows the same area after stripping of the oxide in a solution of 35 cc of 85% phospheric acid and 20g of chromic acid per liter of solution at 80°C. (35). This solution will dissolve the aluminum oxide but will not

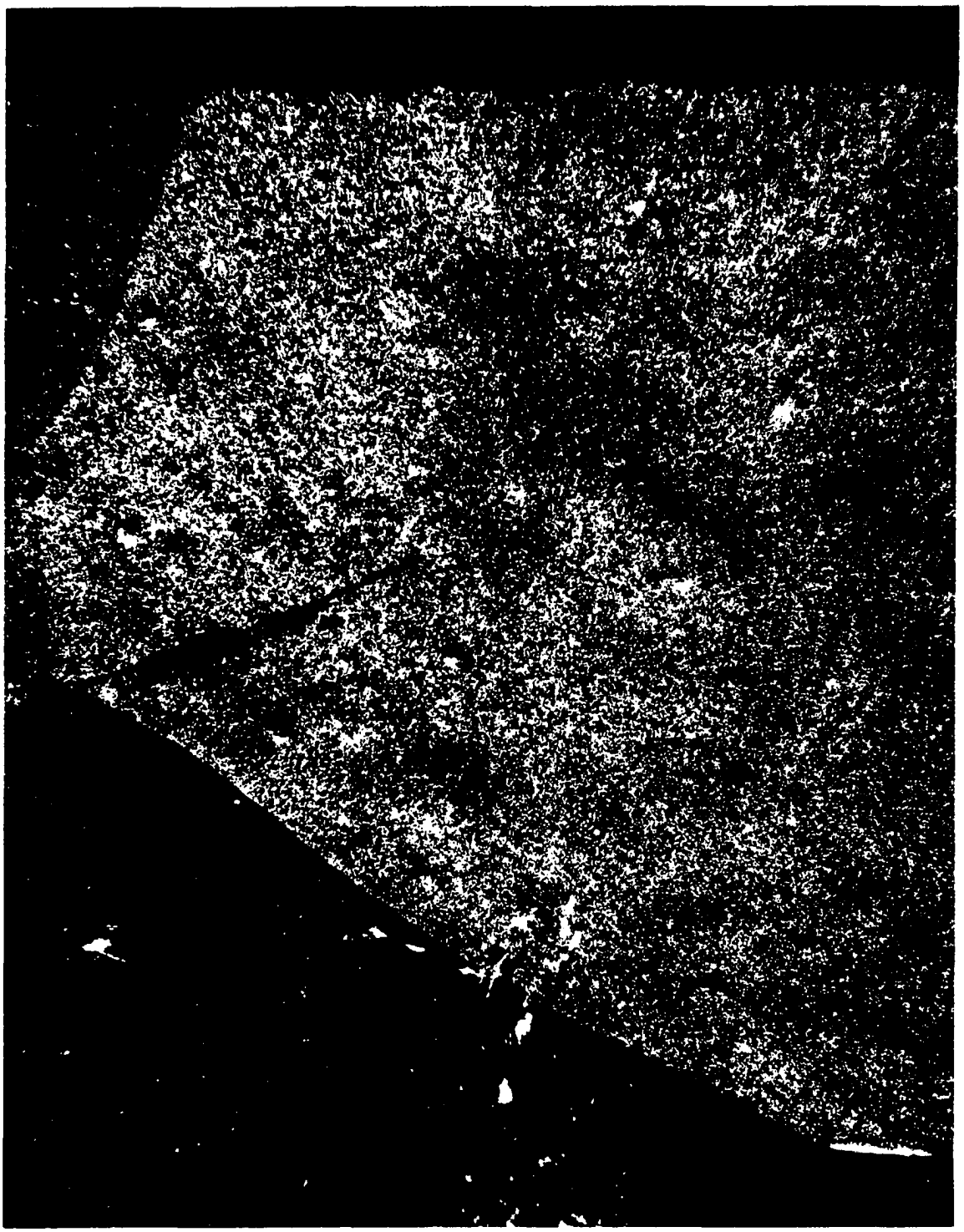

Figure 5. Magnification 50X. High Angle Oblique Illumination. High Purity Aluminum As-Irradiated Condition. 100 Kev Protons. Irradiated Polycrystalline Specimen with Oblique Illumination.

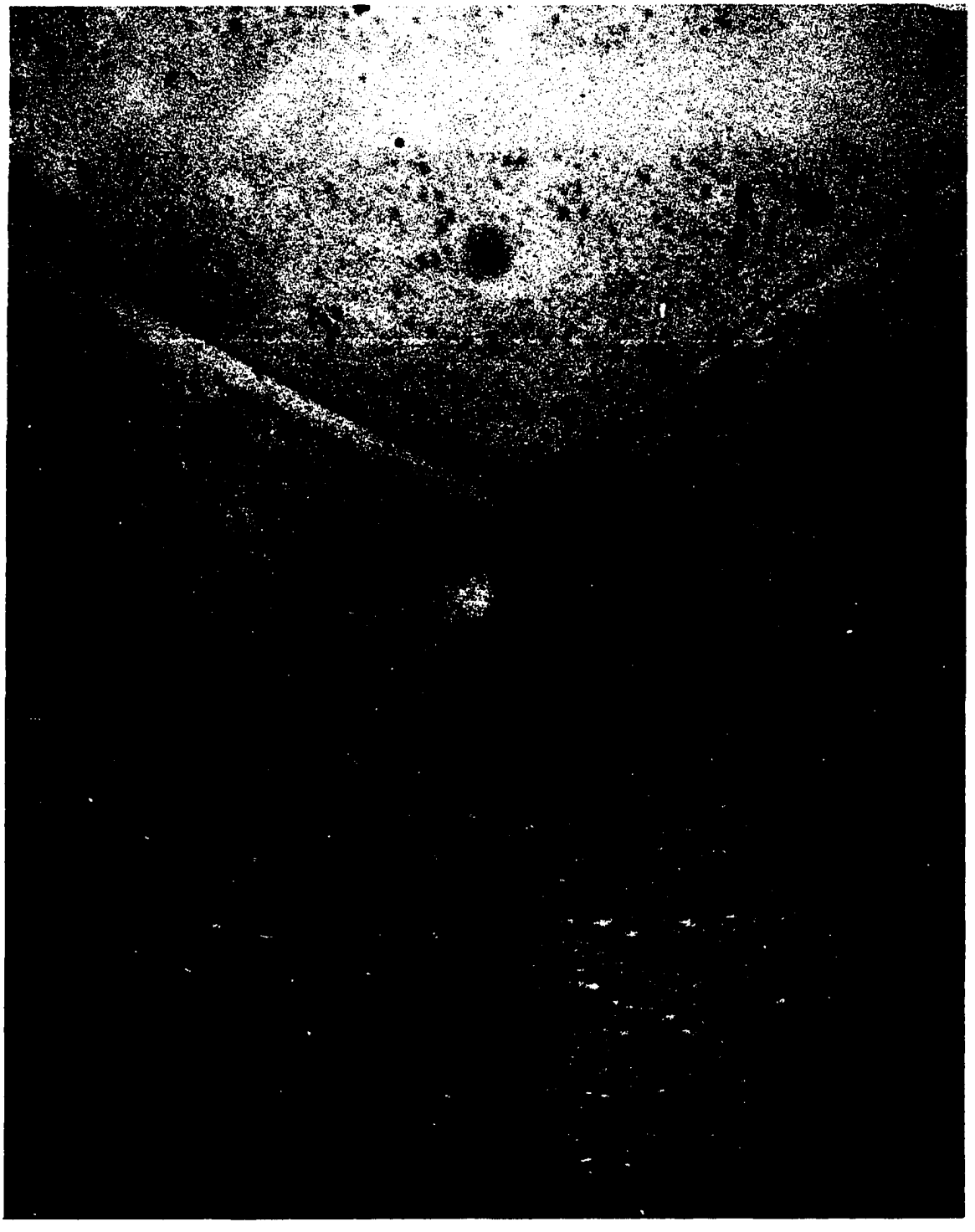

Figure 6. Magnification 1500X. Enlarged 1.8X. Numerical Aperature 1.4. Bright Field Illumination. High Purity Aluminum-As-Irradiated Condition. 100 Kev Protons. Pitting of Oxide on Polycrystalline Specimen.

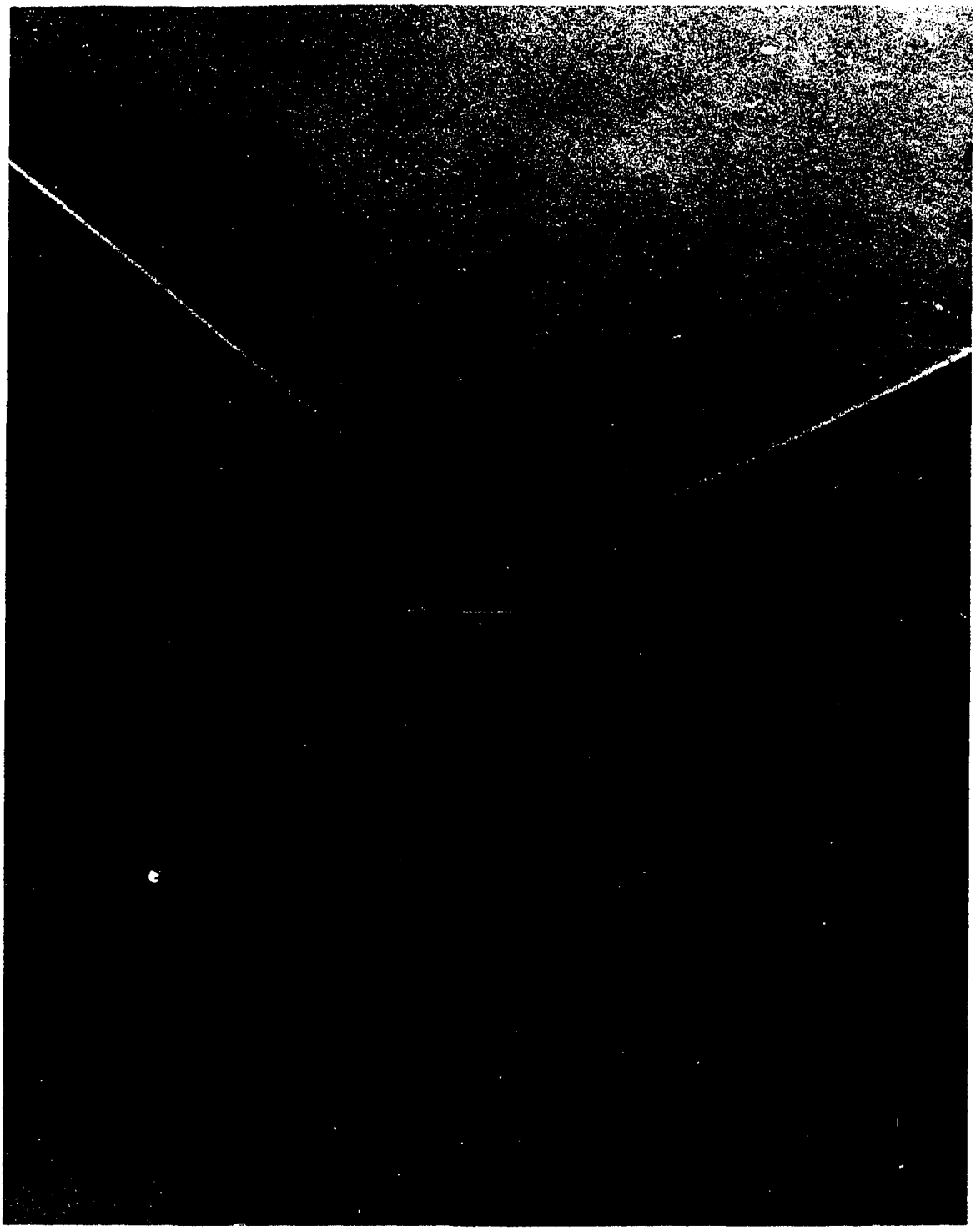

Figure 7. Magnification 1500X. Enlarged 1.8X. Numerical Aperature 1.4. Bright Field Illumination. High Purity Aluminum-As-Irradiated. 100 Kev Protons. Irradiated Polycrystalline Specimen with Oxide Chemically Removed.

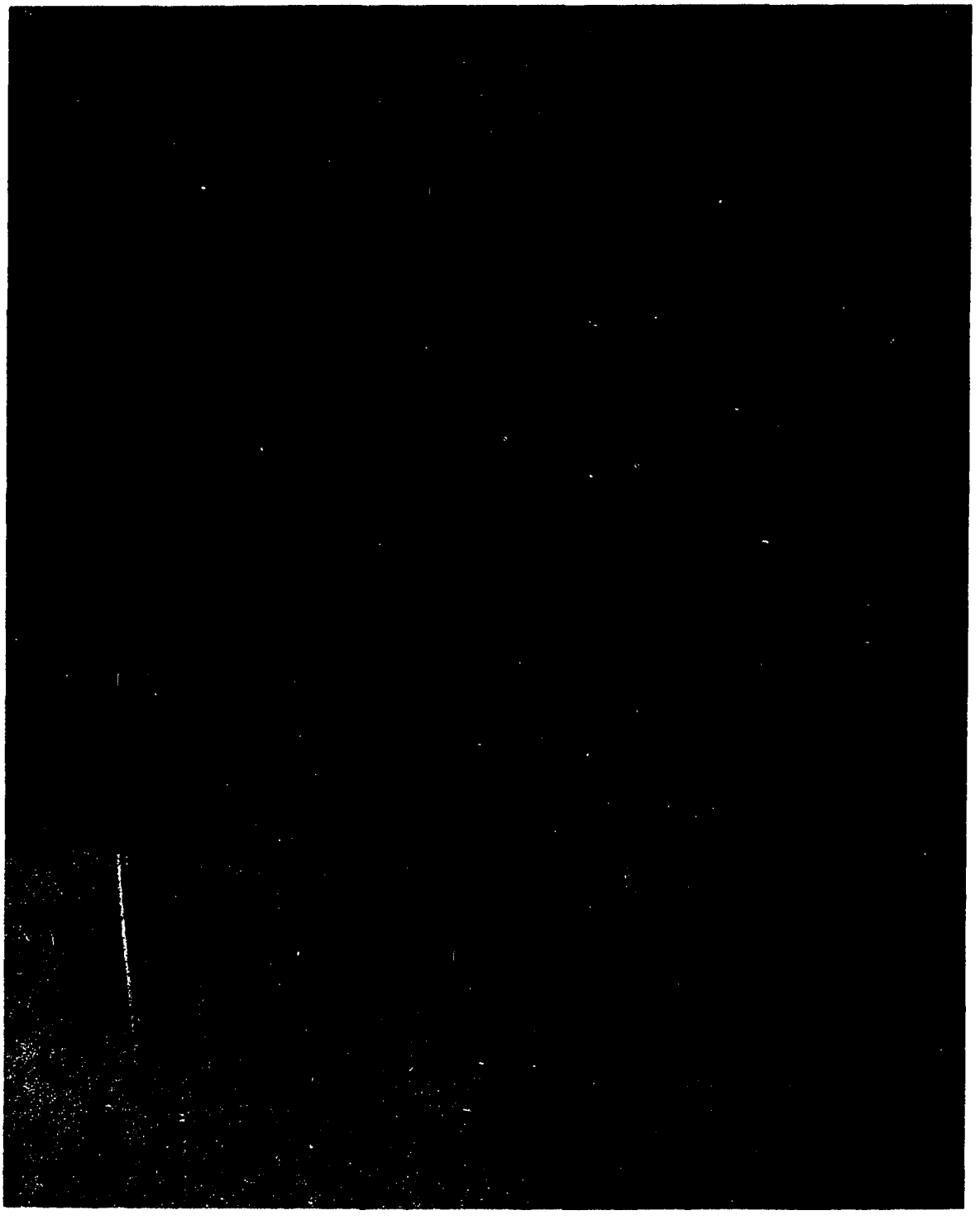

Figure 8. Magnification 1500X. Enlarged 1.8X. Numerical Aperature 1.4. Bright Field Illumination. High Purity Aluminum-Annealed. 100 Kev Protons. Irradiated and Annealed Polycrystalline Specimen with Oxide Chemically Removed.

appreciably attack the aluminum substrate. Chemical stripping of the pitted oxide removed all evidences of the pitting on the aluminum substrate. Figure 8 shows the same area after a ten minute anneal at 300°C. The surface was then blistered. A variation in blister concentration is evident among the three grains. Stripping of the oxide from the blistered surface at this stage produced no change in the surface appearance, i.e., the blisters remained, suggesting that the blisters were not a result of void formation at the oxide metal interface, but are caused by swelling within the matrix. The observations on this one sample show some of the surface effects caused by proton irradiation and illustrate some of the techniques used for observation and analysis of the phenomena.

Pitting of the oxide caused by the bombarding protons was observed at all energies. The degree and distribution of pitting was observed to be affected by particle energy, total flux, crystal orientation, and crystal sub-structure. A general roughening of the metal surface visible under the electron microscope in the areas bombarded by the protons was also observed at all energies (Figure 9). The most obvious pitting damage to the aluminum surface by the proton bombardment was the development of random pits, but within the energy range of 30 to 50 Kev a more complete removal of the oxide from the irradiated area was often noted (Figure 10). The oxide appeared to be removed in large flakes. The degree of pitting was dependent upon the total flux with the amount of pitting and oxide removal by flaking increasing with total flux. This oxide removal process is illustrated in an earlier stage of development in Figure 11.

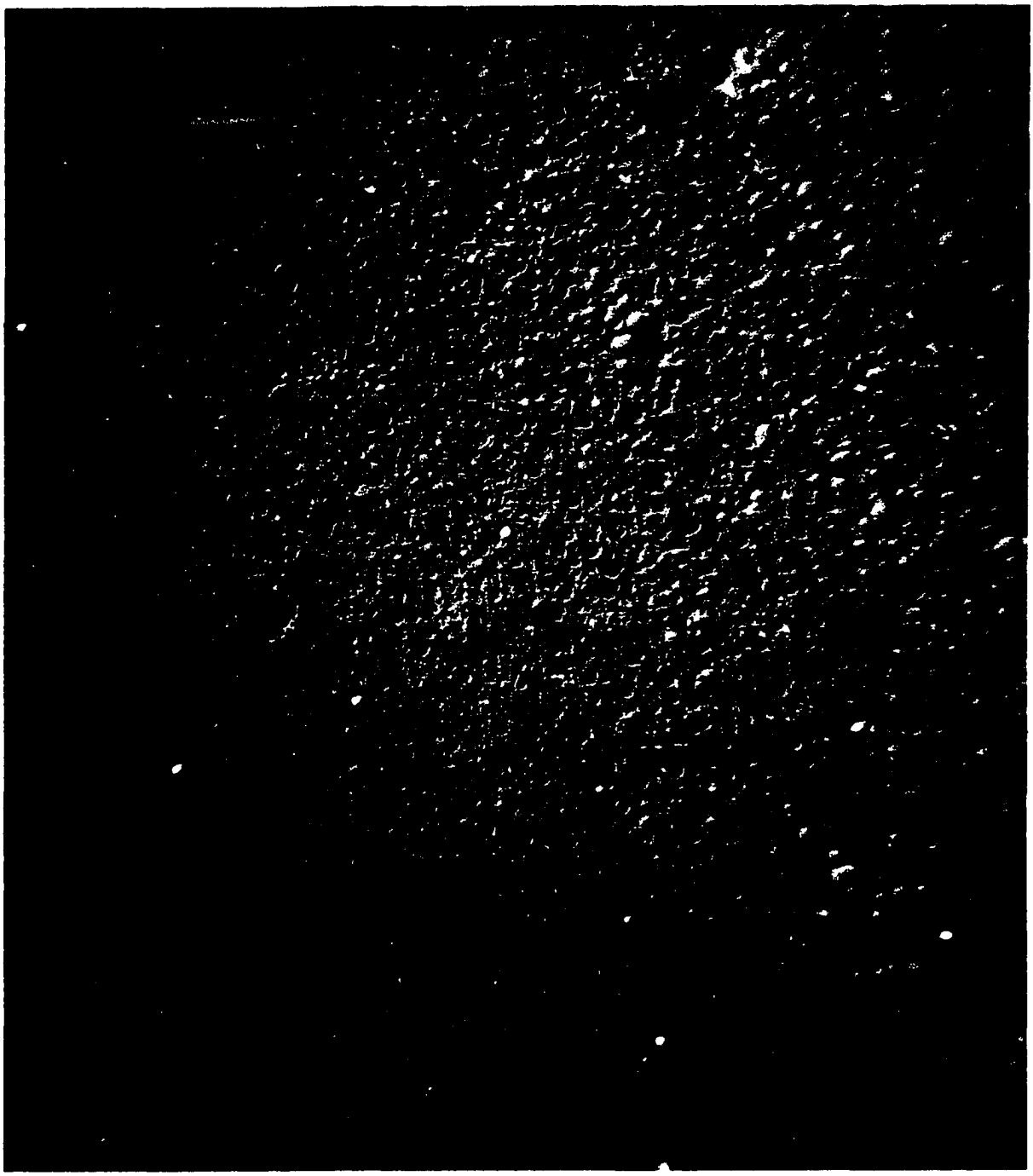

Figure 9. Magnification 11,000X. Electron Micrograph. High Purity Aluminum - Annealed. 100 Kev Protons. Edge of Irradiated Area of Pitted and Blistered Specimen. Irradiated Area is at Upper Right.

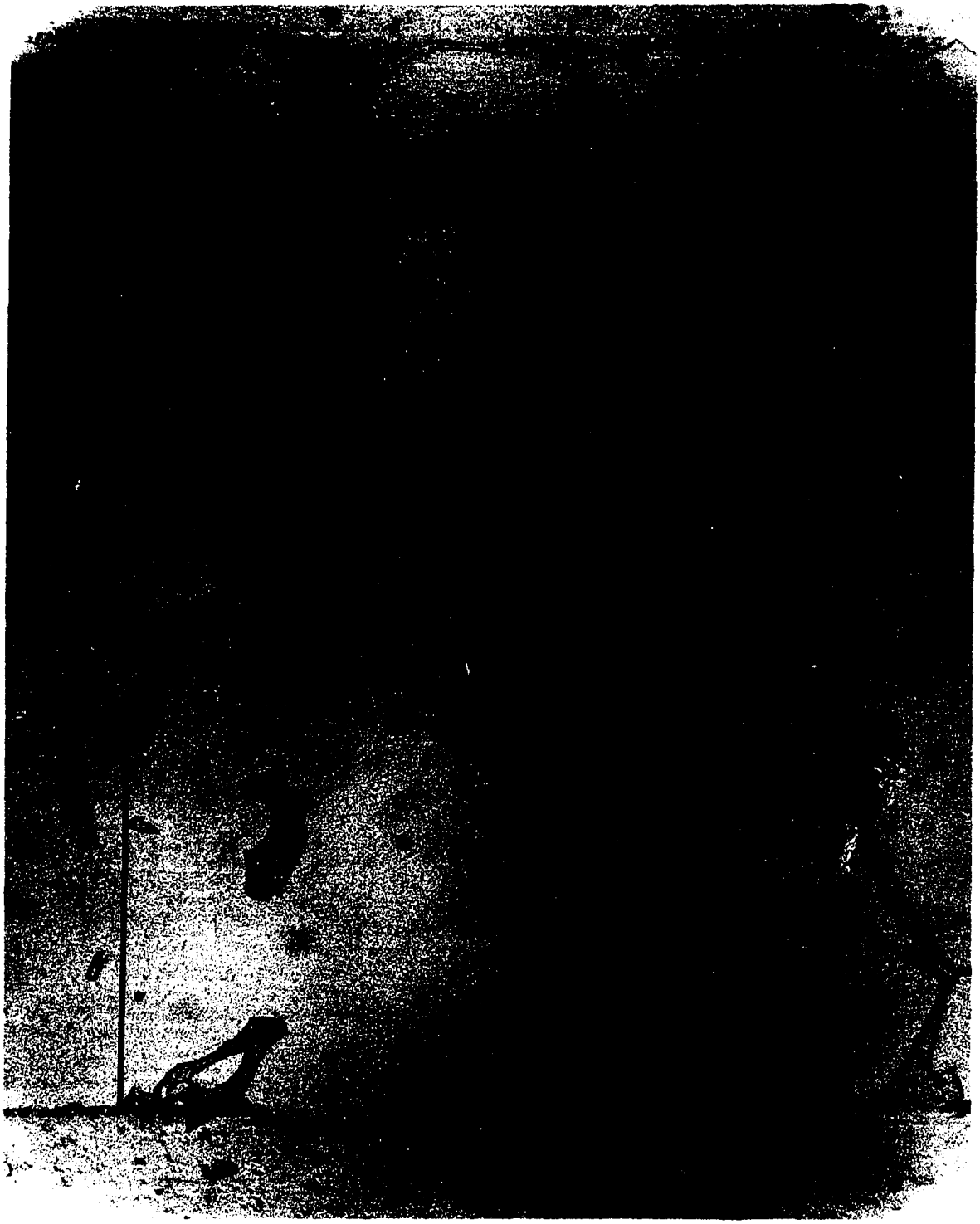

Figure 10. Magnification 240X. Bright Field Illumination.
High Purity Aluminum - As-Irradiated. 50 Kev Protons.
Oxide Removal from Irradiated Area.

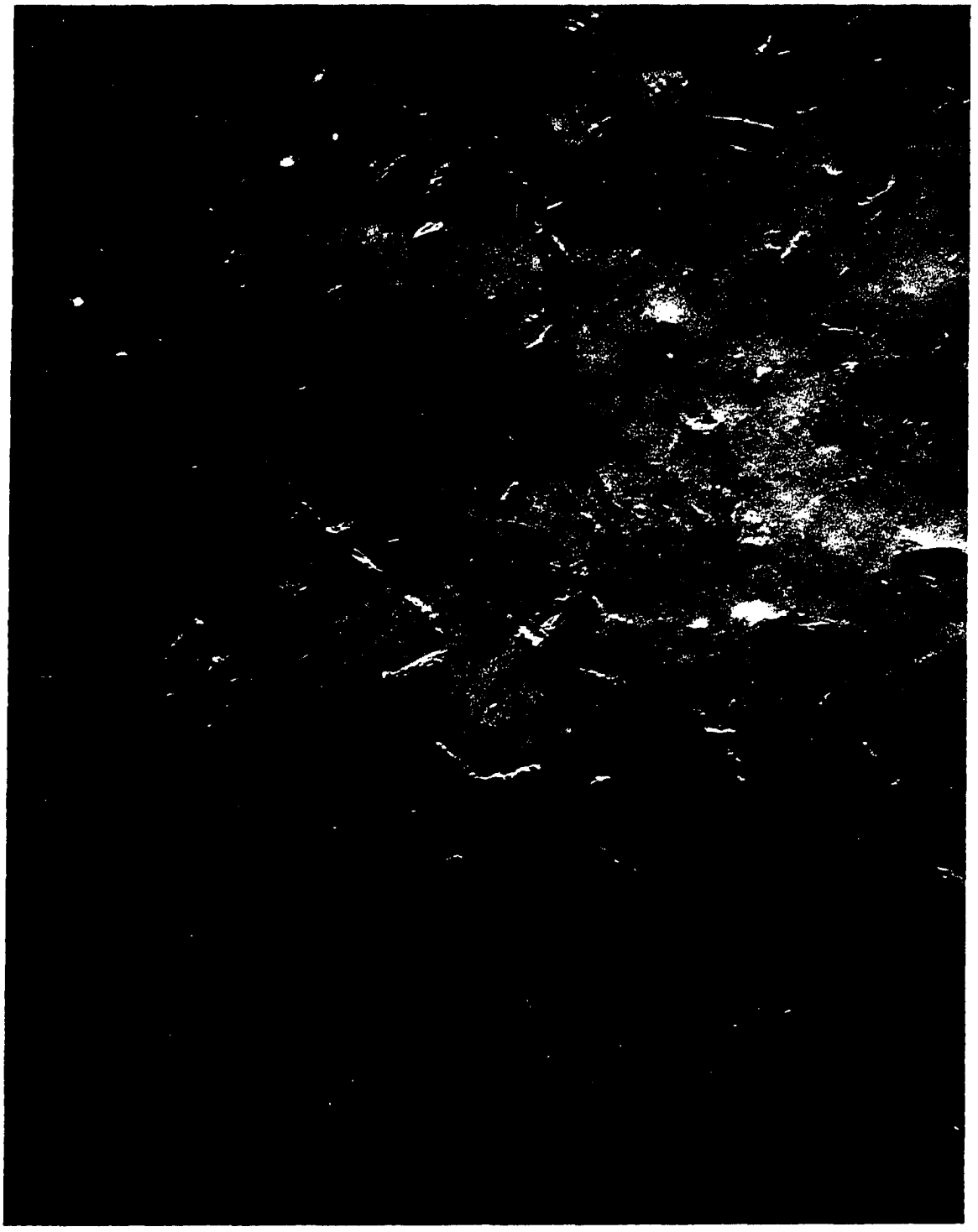

Figure 11. Magnification 240X. Bright Field Illumination.
High Purity Aluminum - As-Irradiated. 50 Kev Protons.
Partial Oxide Removal from Irradiated Area.

The pit concentration, although relatively constant over large areas within each grain, excluding apparent substructure effects, was found to vary among grains. A study of pit concentration versus crystal orientation was conducted utilizing eight polycrystalline specimens. Eight samples each of which contained a number of grains of about 1 mm. diameter were used for this study. The orientation of each individual grain was determined by the Laue back-reflection X-ray technique. The irradiation energies of the specimens were 10, 50, 70, and 100 Kev. There was no detectable variation of pitting tendency among the specimens which could be attributed to differences in incident proton energy. The optical microscope, using oblique illumination at low magnification (75X) and normal illumination at high magnification (1500X), was utilized to determine relative pit concentrations. Pit concentrations versus crystal orientation results are presented in Figures 12, 13, and 16 on a stereographic triangle representation. The crystals whose orientations were close to the (100) and (111) poles show a low pit concentration. The crystal orientations somewhat more removed from these poles show a moderate pit concentration, while the orientations near (110) and the remainder of the stereographic projection triangle show a heavy pit concentration.

The electropolished surface of high purity aluminum irradiated with 50 to 450 Kev protons was observed under the optical microscope to blister if the total flux was above a lower limit of approximately 5×10^{16} p/cm^2. This large scale blistering occurred spontaneously for irradiations at energies of 50 to 70 Kev but occurred only upon annealing at temperatures of 250°C. or above on specimens irradiated with 100

to 450 Kev protons. The distribution and degree of blistering was observed to be affected by cold working, crystal orientation, and crystal substructure.

A study was made of the variation of blister concentration with crystal orientation in a manner similar to that for pit concentration versus crystal orientation. The samples from the previous pit concentration study were utilized with the exception of the 10 Kev specimen which showed no blistering under the optical microscope. The samples were first treated with the oxide stripping solution which removed the pitting. The samples were then annealed at 300°C. to produce full development of blisters. The optical microscope with high angle oblique illumination and normal illumination was again utilized to determine relative blister concentrations. The results of this study are presented in Figures 14, 15, and 17. A light blister concentration is associated with crystals whose orientation lies near the (111) pole, and a moderate blister concentration is associated with crystals near the (100) pole and those crystals somewhat more removed from the (111) pole. The orientations in the remainder of the stereographic triangle possessed a heavy blister density.

The distribution of blisters within single grains of some samples were found to be non-uniform with a heavy concentration of blisters along hexagonal or lamaller shaped subgrain boundaries. This phenomenon occurred in single crystals grown from the melt. Figure 18 shows a heavy blister concentration associated with a 100 micron hexagonal substructure in a crystal grown from the melt by the Bridgeman technique. The existence of this substructure, probably associated with a segregation of impurities to selective regions of the material during uniaxial solidification, could

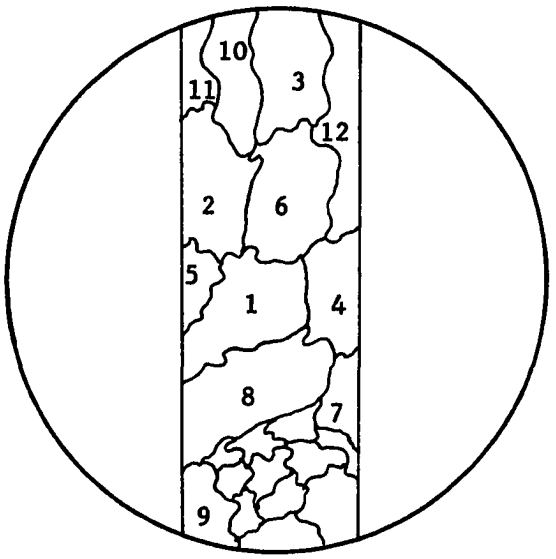

(A) Representation of Irradiated Grains

HEAVY	MEDIUM	LIGHT
4	5	1
6	9	2
7	10	3
8	11	

(B) Classification of Degree of Pitting

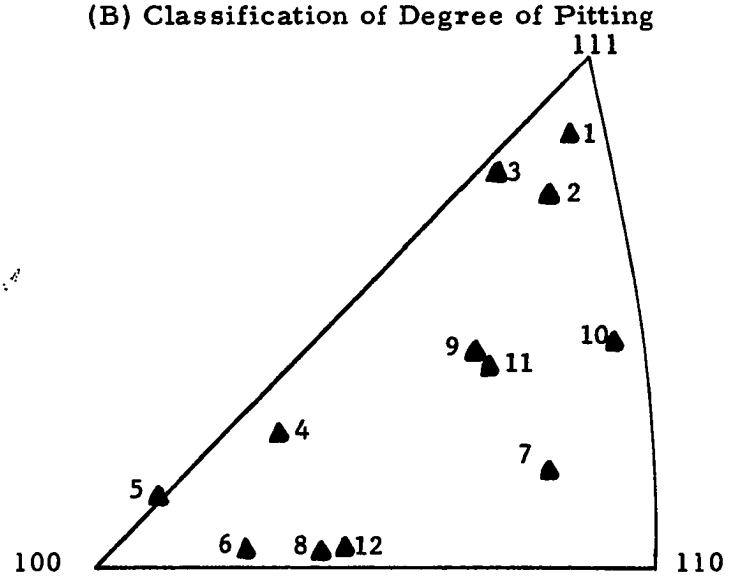

(C) Grain Orientations Plotted on Stereographic Triangle

Figure 12-- Identification, Classification and Orientation of Grains within Irradiated Region. Classification is based upon degree of pitting.

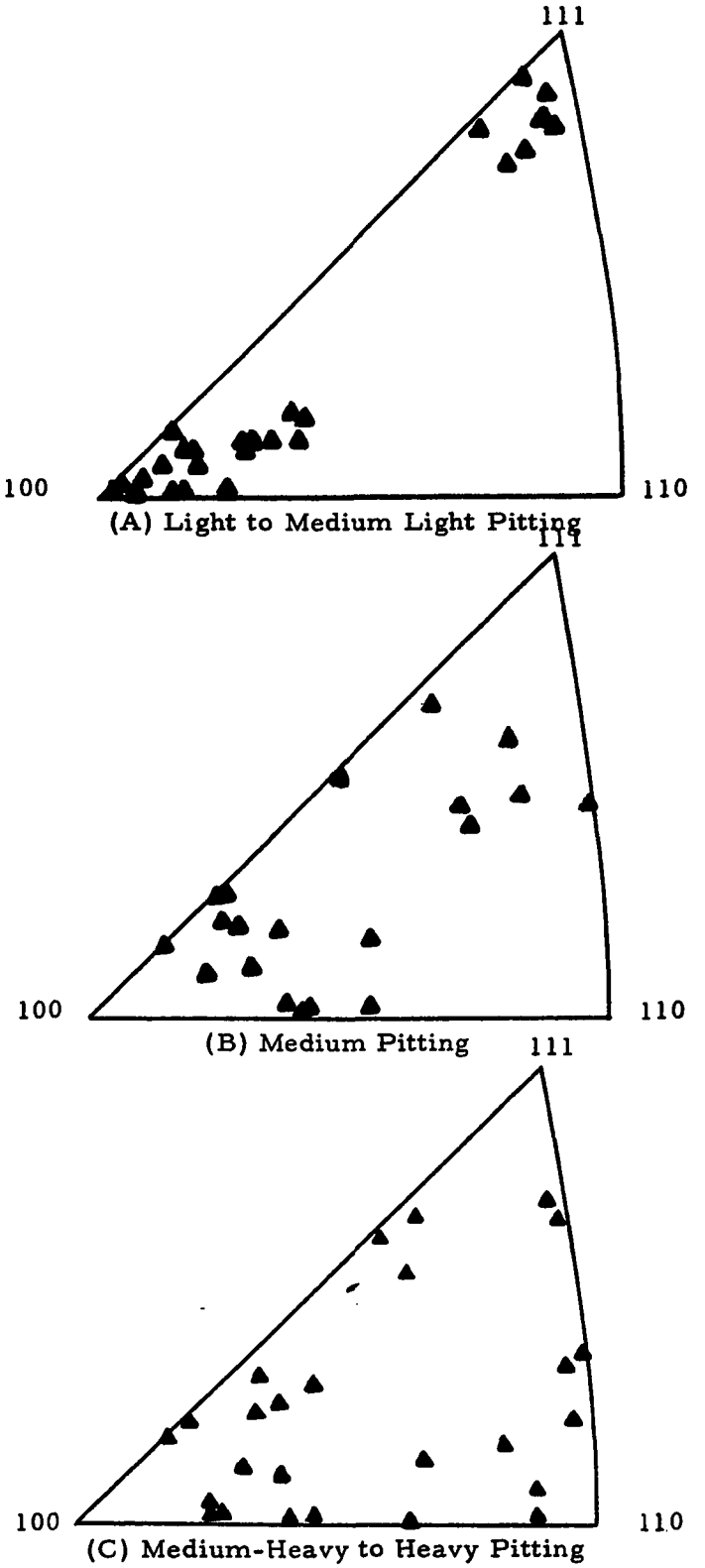

Figure 13-- Orientation of Grains Based Upon Classification According to Degree of Pitting.

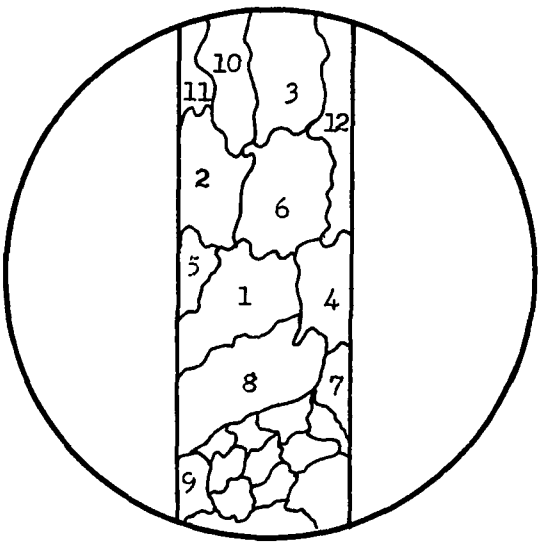

a. Representation of Irradiated Grains

Light	Medium	Medium to Heavy
1	5	4 10
2	6	7 11
3		8 12
		9

b. Classification of Degree of Blistering

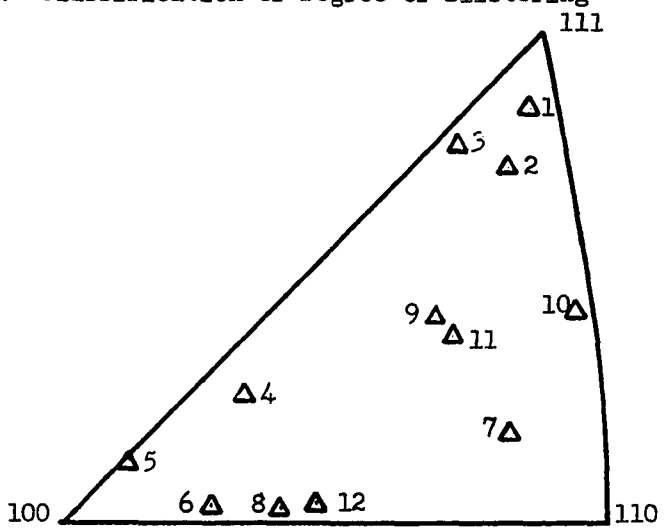

c. Grain Orientations Plotted on Stereographic Triangle

Figure 14. Identification, Classification and Orientation of Grains within Irradiated Area. Classification is based upon degree of blistering.

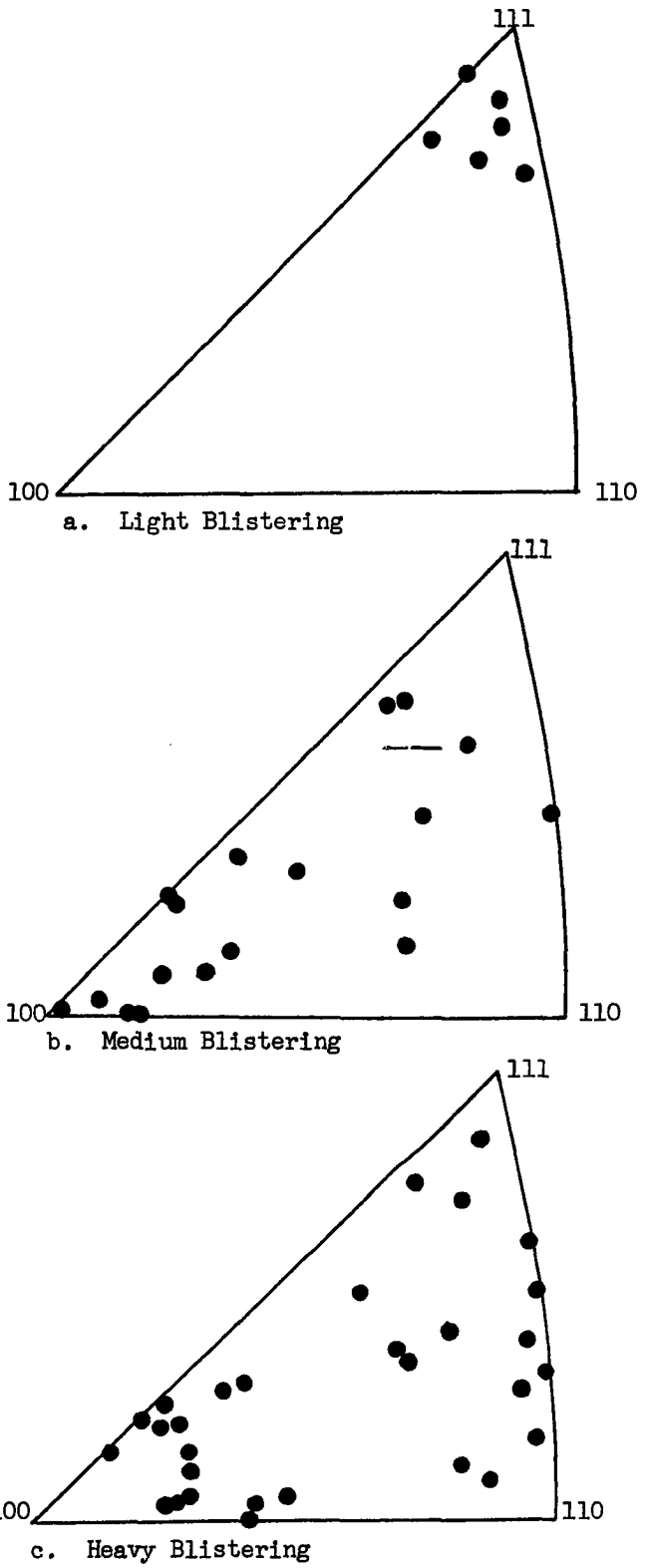

Figure 15. Orientation of Grains Based upon Classification According to Degree of Blistering.

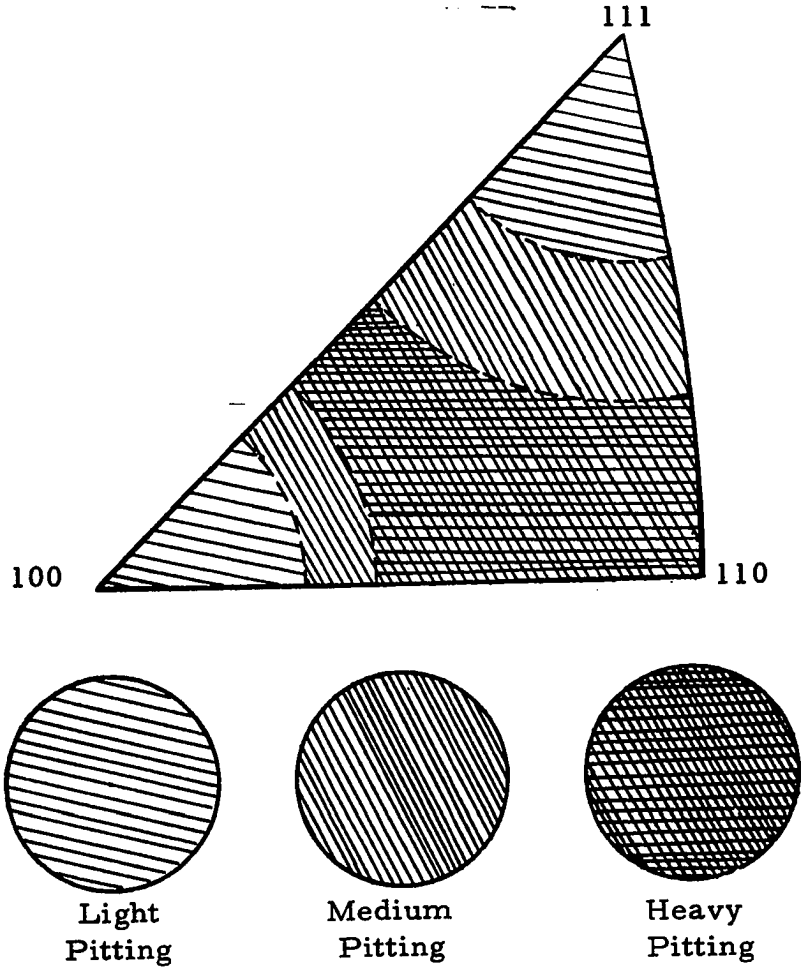

Figure 16-- Composite Diagram Showing Orientations of Light, Medium, and Heavy Pitting Represented as Areas on Stereographic Triangle.

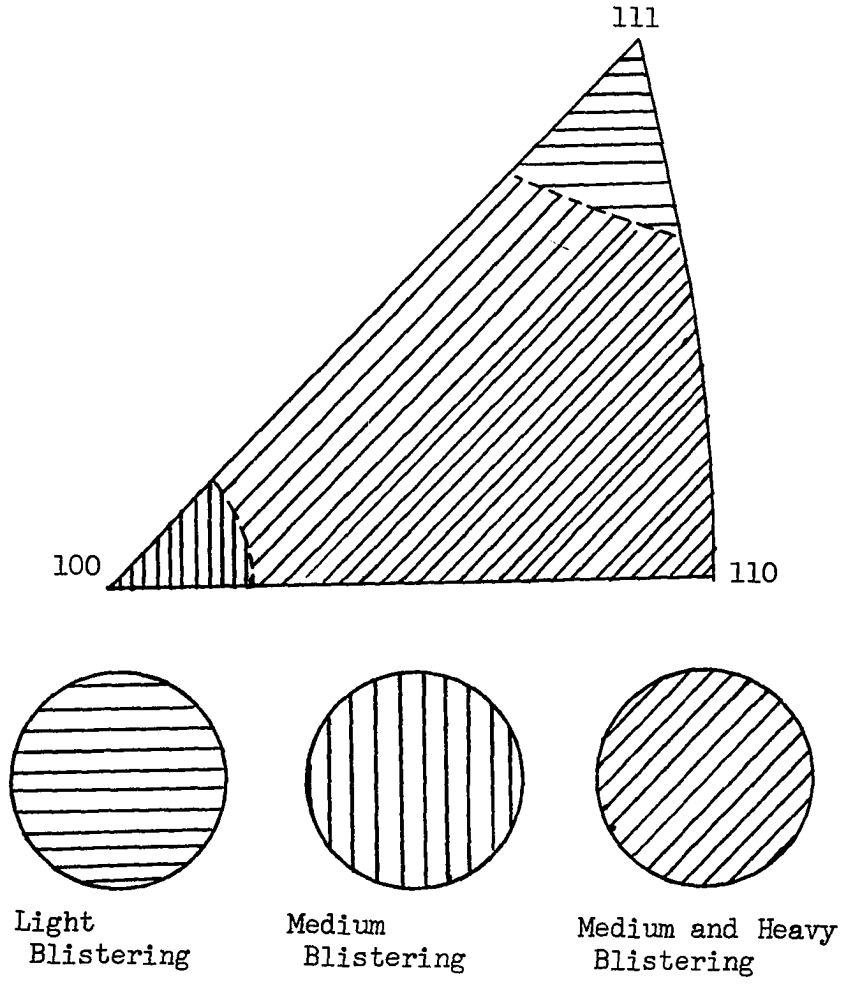

Figure 17. Composite Diagram Showing Orientations of Light, Medium, and Heavy Blistering Represented as Areas on Stereographic Triangle.

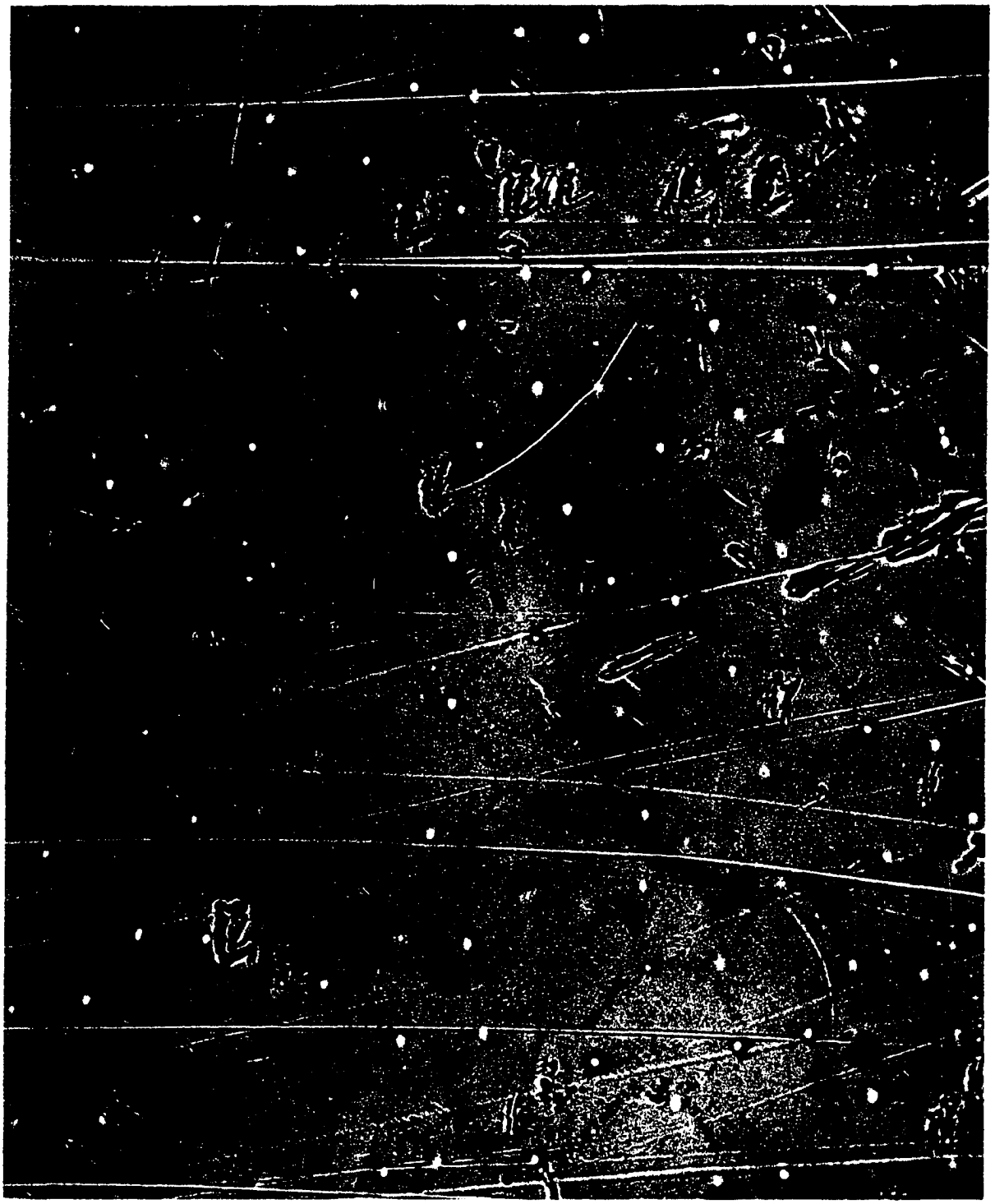

Figure 18. Magnification 265X. Bright Field Illumination. High Purity Aluminum - Annealed. 100 Kev Protons. Blisters along Hexagonal Structure Associated with Impurity Segregation.

also be delineated in the material by an excessive electropolish. This treatment caused pitting of the aluminum surface in the impurity segregation regions. As an example of this technique, Figure 19 shows a lamaller impurity structure in a tricrystalline specimen grown from the melt. No evidence could be found of an excessive pitting of the aluminum oxide in the region of this impurity structure.

A 75-80 micron hexagonal structure associated with a heavy blister concentration and a heavy pitting concentration was found in recrystallized aluminum which had been irradiated and subsequently annealed. No explanation as to the factors causing this substructure in recrystallized aluminum could be given from the experimental observations. Figure 20 shows a heavy pit concentration associated with the structure in the recrystallized material; the heavy blister concentration on a sample from which the oxide was stripped appeared identical when viewed under high angle oblique illumination. The boundaries of heavy pit distribution coincided with the boundaries of heavy blister distribution.

In an effort to determine if the effects observed above could be attributed to a dislocation substructure in the recrystallized aluminum specimens, a series of chemical dislocation etching treatments were conducted. A study of the literature produced various solution treatments for aluminum represented as being capable of delineating dislocation substructures by selective dislocation etch pit formation (37-39). Etching treatments were successful in delineating most of the dislocation substructures reported in the literature as having been observed in aluminum plus variations which could not be found in the literature, but no structures similar to the 75-80 micron hexagonal pattern shown in

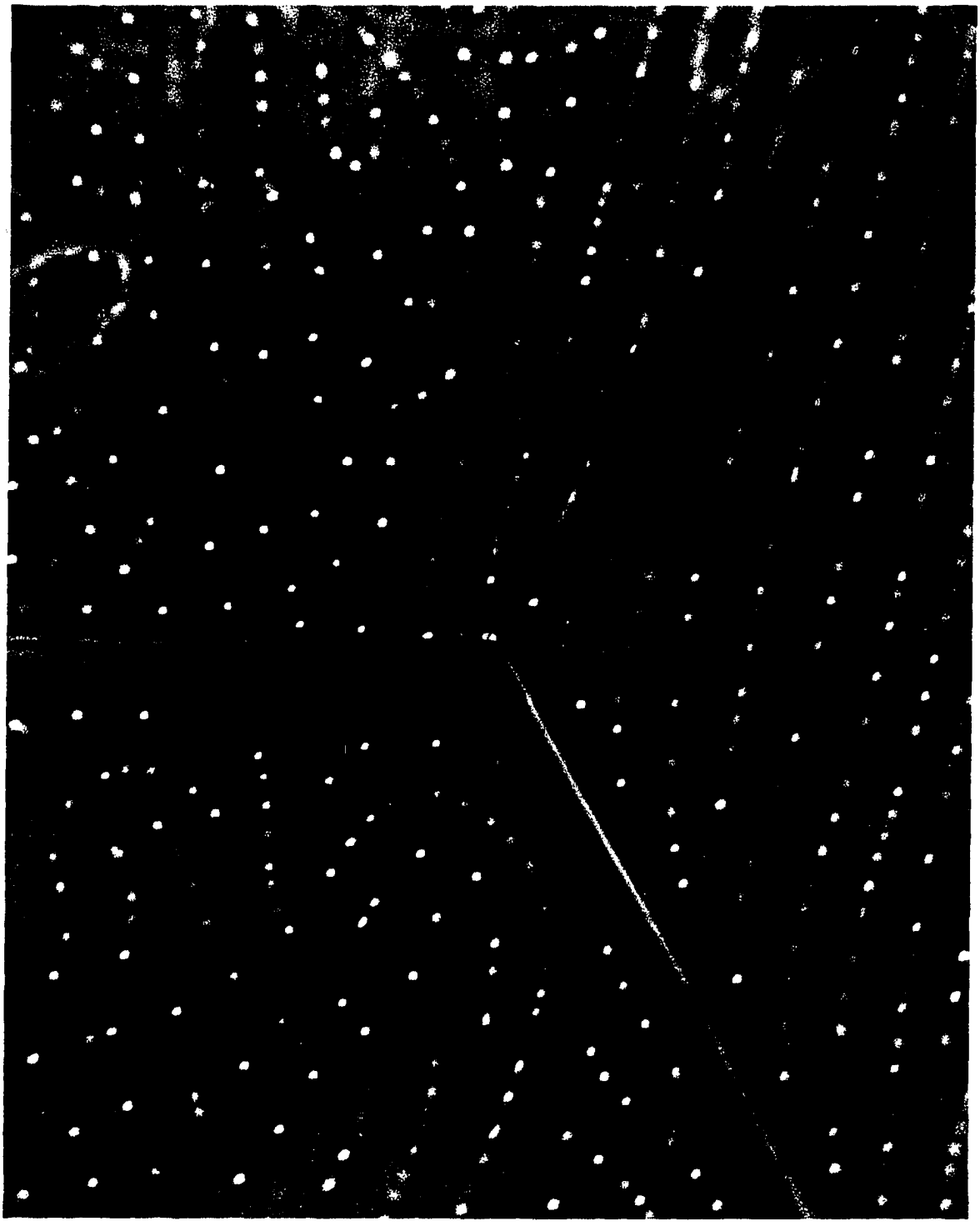

Figure 19. Magnification 80X. Bright Field Illumination. High Purity Aluminum - Unirradiated. Delineation of Impurity Segregation Structure by Excessive Electropolishing.

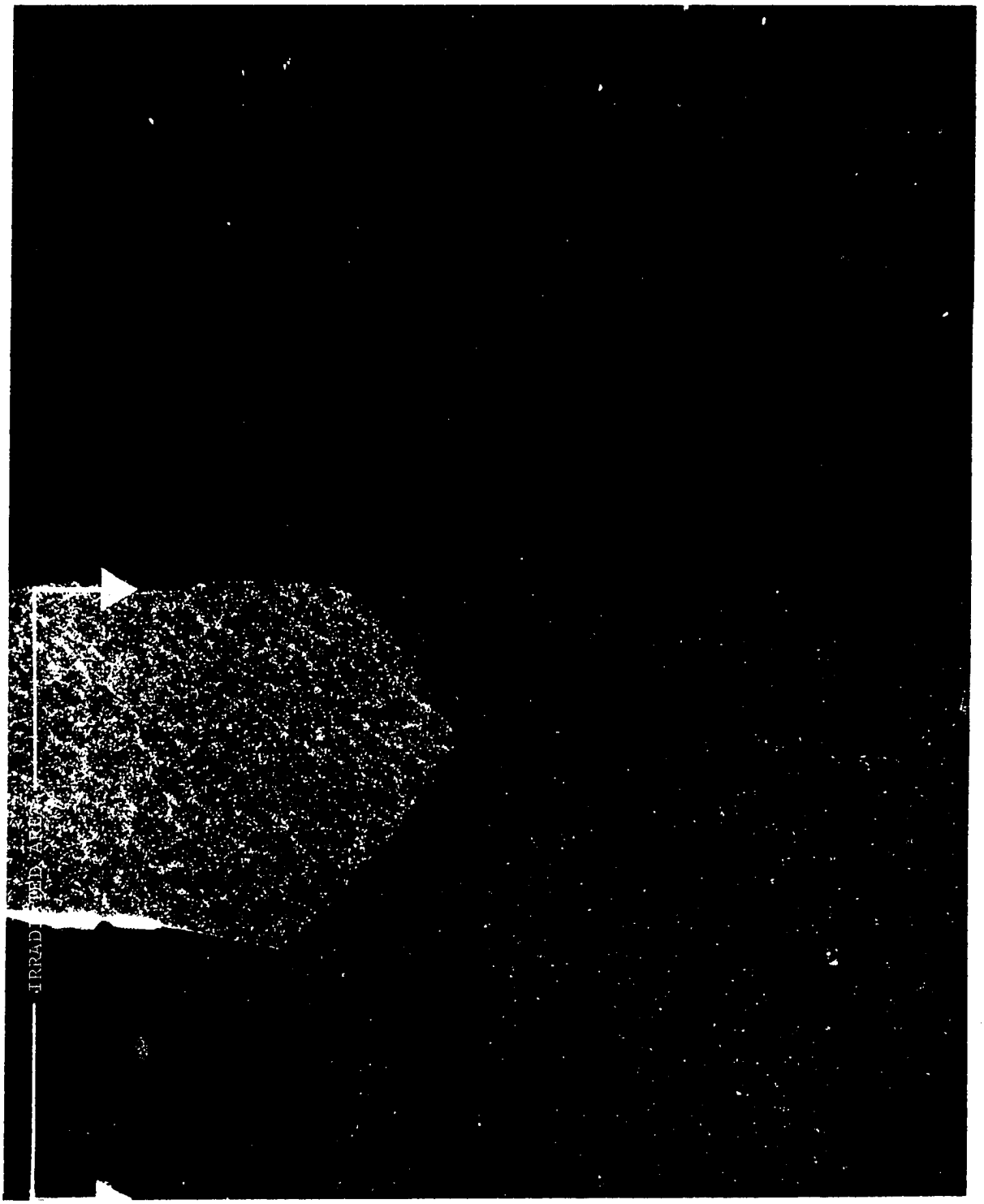

Figure 20. Magnification 120X. High Angle Oblique Illumination. High Purity Aluminum - As-Irradiated. 100 Kev Protons. Pitting along Substructure in Recrystallized Aluminum. Area at Top is Unirradiated.

Figure 20 were found. An attempt to delineate the 100 micron impurity substructure or the impurity lamaller structure, obtained in aluminum crystals grown from the melt, with dislocation etch pit solutions was similarly unsuccessful.

Observation of electropolished aluminum also revealed an apparent structure in the oxide (Figure 21). Similar structures observed by other investigators have been attributed to the electropolishing process (40-41). Examination of blistered and pitted irradiated samples on an optical microscope revealed no correlation between the geometry or location of the blisters and pits and this oxide structure. These results are not considered conclusive because of the low resolution capability of the optical microscope.

Examination of irradiated polycrystalline aluminum with the optical microscope has shown instances of blistering and pitting being selectively excluded from along portions of the grain boundary of some grains (Figures 6 and 8). The width of these blister and pit free regions varied along different boundaries with an average width of 2 to 5 microns. A more detailed study with the electron microscope has revealed the existence of very small scale blistering and pitting along the boundary (Figures 22-23), with a corresponding pit or blister free region adjacent to the boundary. This behavior is somewhat analogous to formation of a depletion zone adjacent to a grain boundary sink. This behavior did not occur in all grain boundaries in the irradiated zone. No attempt was made to determine a correlation of this grain boundary effect with crystal orientation due to the inconsistency of its occurrence.

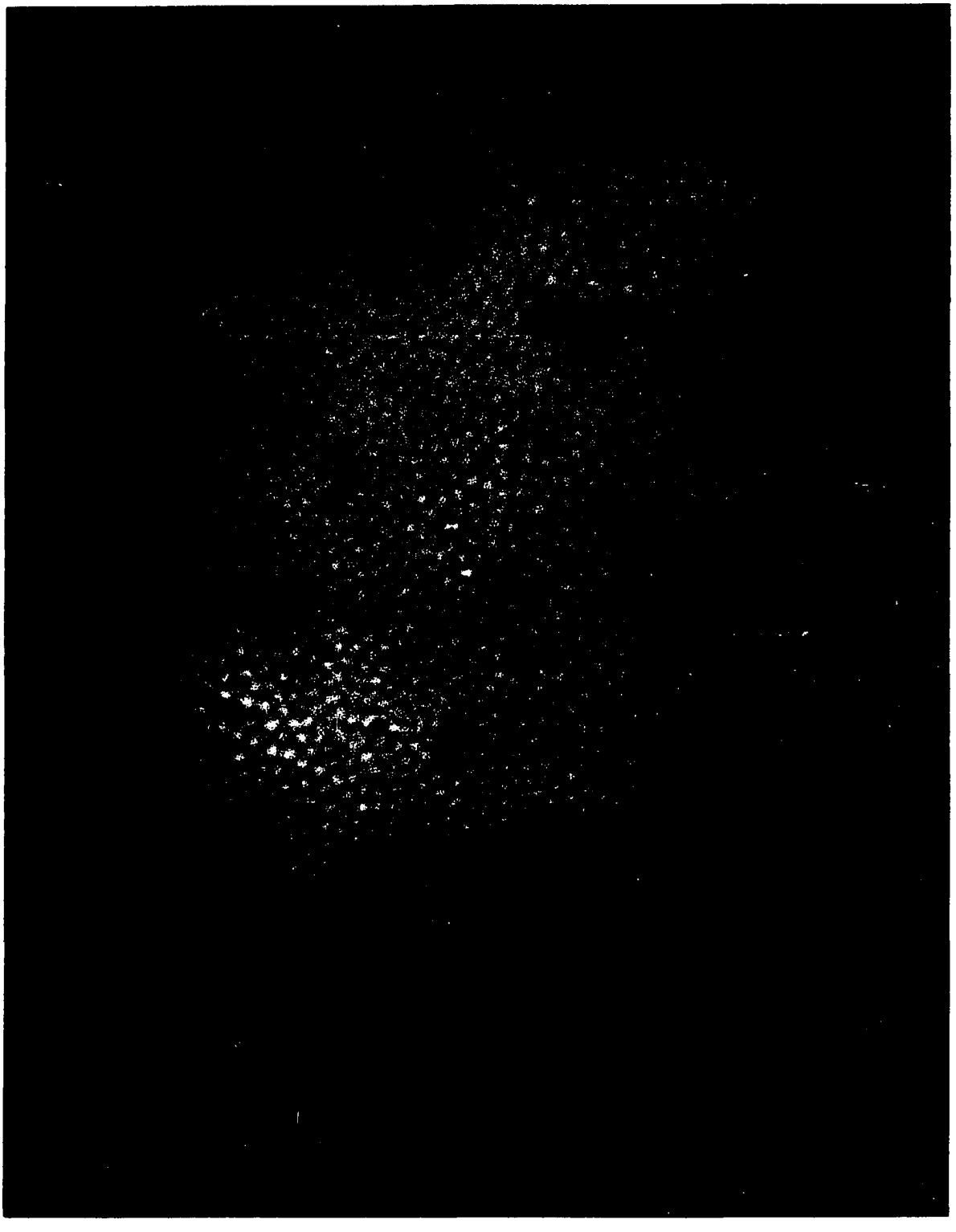

Figure 21. Magnification 730X. Bright Field Illumination.
High Purity Aluminum - Unirradiated.
Structure in the Oxide due to Electropolishing.



Figure 22. Magnification 11,000X. Electron Micrograph.
High Purity Aluminum - Annealed with Oxide Chemically Stripped. 50 Kev Protons.
Elongated Blisters. Some of which have Collapsed.
Heavy Blister Concentration along Grain Boundary.



Figure 23. Magnification 11,000X. Electron Micrograph. High Purity Aluminum - Annealed. 100 Kev Protons. Limited Degree of Pitting and Blistering along Grain Boundaries.

Study of proton irradiated aluminum alloy was quite limited. Alloys were used in some of the preliminary experiments, but their use was discontinued when it became apparent that microstructural factors were of significant importance in the manner and occurrence of blisters and that characterization of the blister phenomenon with material of as high a purity as obtainable was a necessary starting point in the investigation. However, comparison of the blistering and pitting of alloys with behavior in high purity material is quite instructive. Blistering of the alloy material occurred in a manner similar to that observed in the high purity aluminum with regard to irradiation parameters and behavior upon annealing. In Figure 4 is shown an irradiated and annealed 6061 alloy specimen. This specimen was irradiated with a 200 Kev unanalyzed beam.* The most impressive aspect of the observed blistering was the blister size which was considerably larger than that observed in pure aluminum. Also, elongation of the blisters in the direction of rolling striations illustrates an effect of cold working upon blister geometry.

The effects of cold working the surface on the distribution and size are quite graphically illustrated on a sample whose surface was inadvertantly scratched shortly after irradiation with protons. It was observed that blisters on the surface of the high purity aluminum sample which contained a region cold worked by scratching were larger in the cold worked region than elsewhere and were oriented with the direction of the deformation (Figures 24A and 24B). Figure 24A was taken after a

---

*Initial studies prior to this research were conducted with an unanalyzed irradiation particle beam. This beam was composed of H^+, H_2^+, and H_3^+ ions in approximate proportions of 48:32:20.

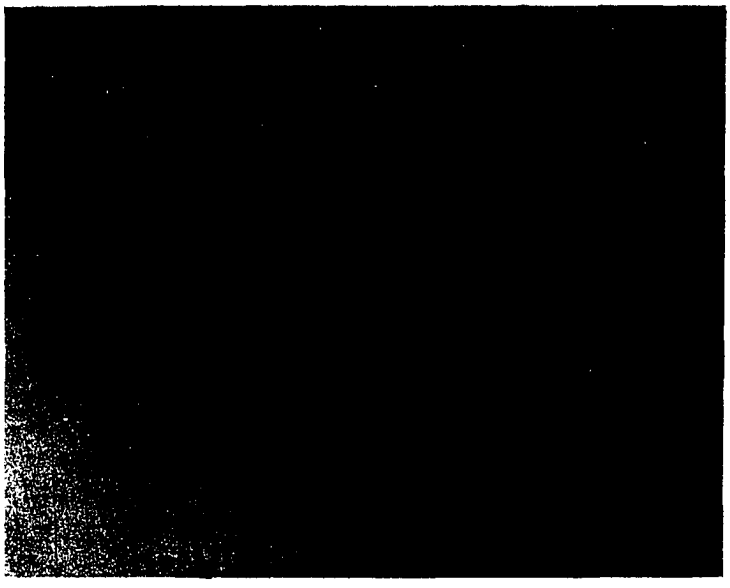

24A. After 20 min. anneal at 250°C.

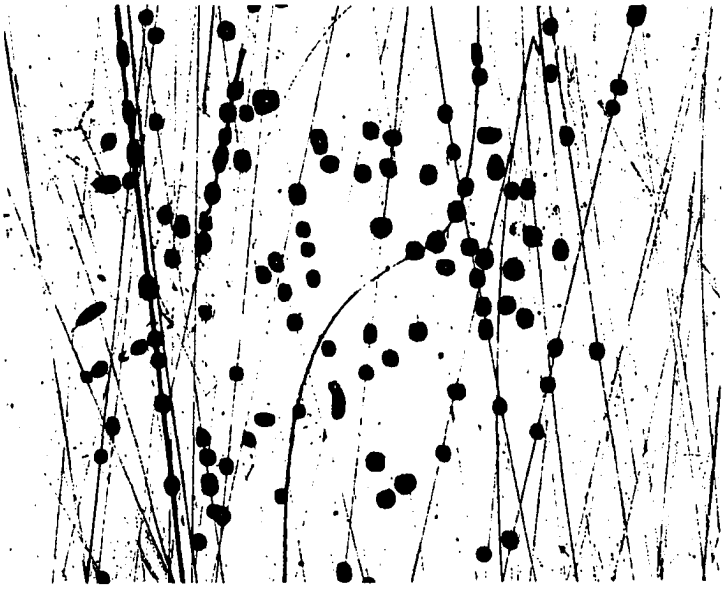

24B. Area shown in 24A after further Annealing for 10 min at 350°C.

Figure 24. Magnification 150X. Bright Field Illumination. High Purity Aluminum-Annealed. 100 Kev Protons Large Blisters Situated along Scratches.

twenty minute anneal at 250°C. and Figure 24B after a further ten minute anneal at 350°C. These figures represent substantially the same area on the sample. Of particular interest is the alignment of the blisters along the gouge marks and the greater blister density following the higher temperature anneal. This was the only sample for which an increase in blister density with increased annealing time and temperature was recorded photographically.

Several irradiated aluminum specimens were annealed in a vacuum hot stage furnace. Optical observation of the irradiated area, while the specimens were held at temperature, was intended to provide information concerning the kinetics of the blistering process. However, this technique provided only limited information concerning the formation and growth of individual blisters. The small size of the blisters obtained on high purity material made it impossible to resolve them using the 40X long working distance objective provided for use with the vacuum hot stage. Upon heating the specimen to 250°C. all that could be observed was a darkening of the irradiated surface. As the temperature was increased or as time progressed the darkening increased until it reached a maximum. Further heating to a maximum temperature of 350°C. reduced the degree of this darkening until some constant optical condition was reached. Examination of the irradiated surfaces upon removal of the specimens from the vacuum hot stage furnace showed this darkening was caused by blistering of the surface.

Aluminum specimens cooled to -200°C. or heated to +200°C. were bombarded with 100 Kev protons. No pitting was observed on these samples in the as-irradiated condition. Annealing at 300°C. produced a heavy

concentration of blisters on the specimens irradiated at -200°C. but produced no blistering on the specimens irradiated at +200°C. These results appear to be consistent with the mechanisms proposed for these processes.

Gold samples were irradiated with 50 and 100 Kev protons to integrated fluxes of 10^{17} protons/cm^2. Although a small change of the surface reflectance characteristics in the irradiated area was usually observed, examination with the optical microscope failed to reveal the cause of this variation. Annealing of the gold specimens at 300°C. for ten minutes produced blistering upon the 100 Kev irradiated specimen (Figures 25 and 26). This observation is not conclusive, however, since some grains possessed a very poor initial surface finish. Although blisters were observed upon all grains, the poor quality of surface finish of some grains did not permit an accurate determination of the relative blister concentration among all grains in the irradiated area. This variation of the surface finish among grains is attributed to a grain orientation dependence of the electropolishing response for the process utilized for surface preparation of the high purity gold specimens.

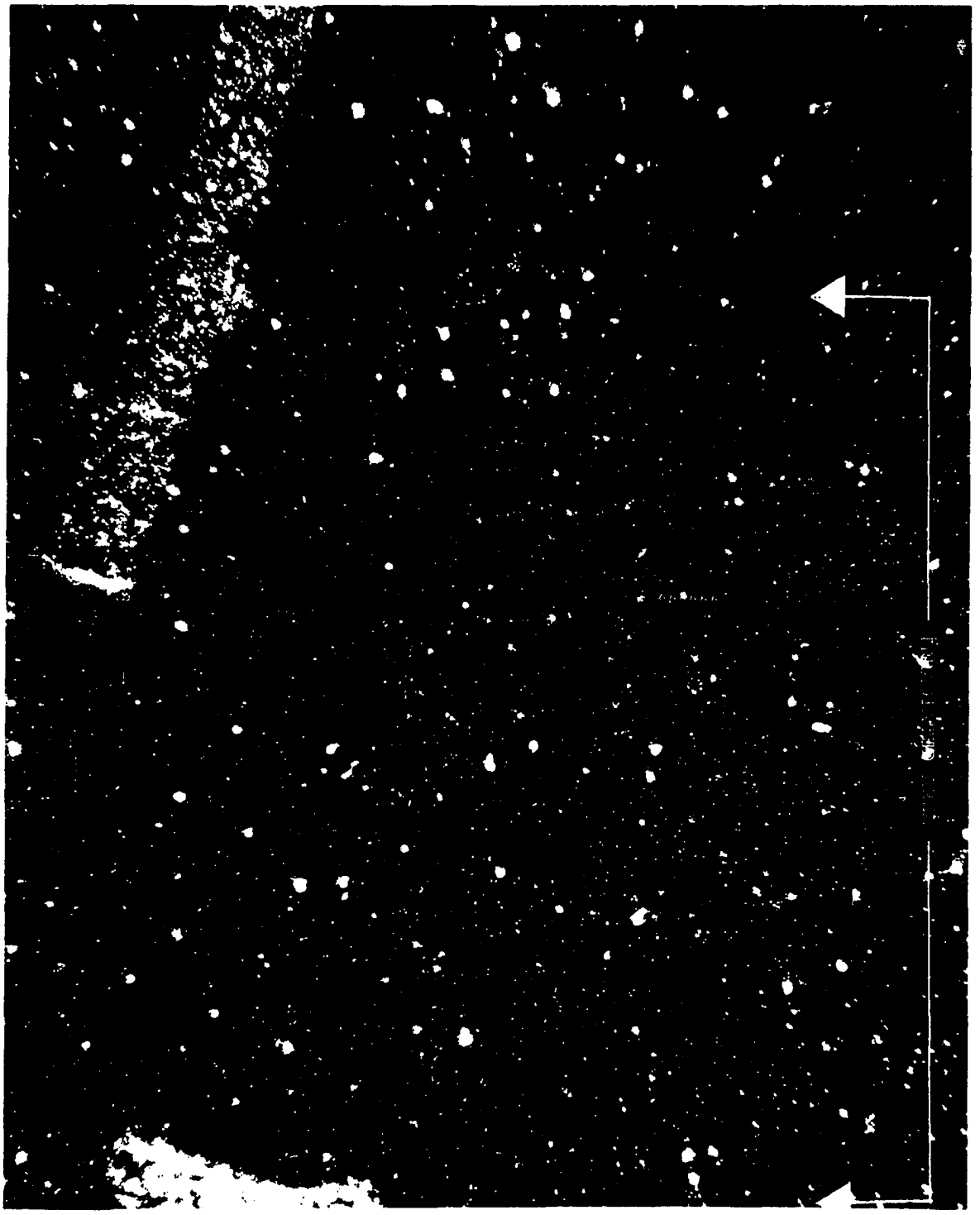

Figure 25. Magnification 120X. High Angle Oblique Illumination. High Purity Gold-Annealed. 100 Kev Protons. Diffuse Scattering of Light Associated with Blisters in Irradiated Area. Area at top is Unirradiated.

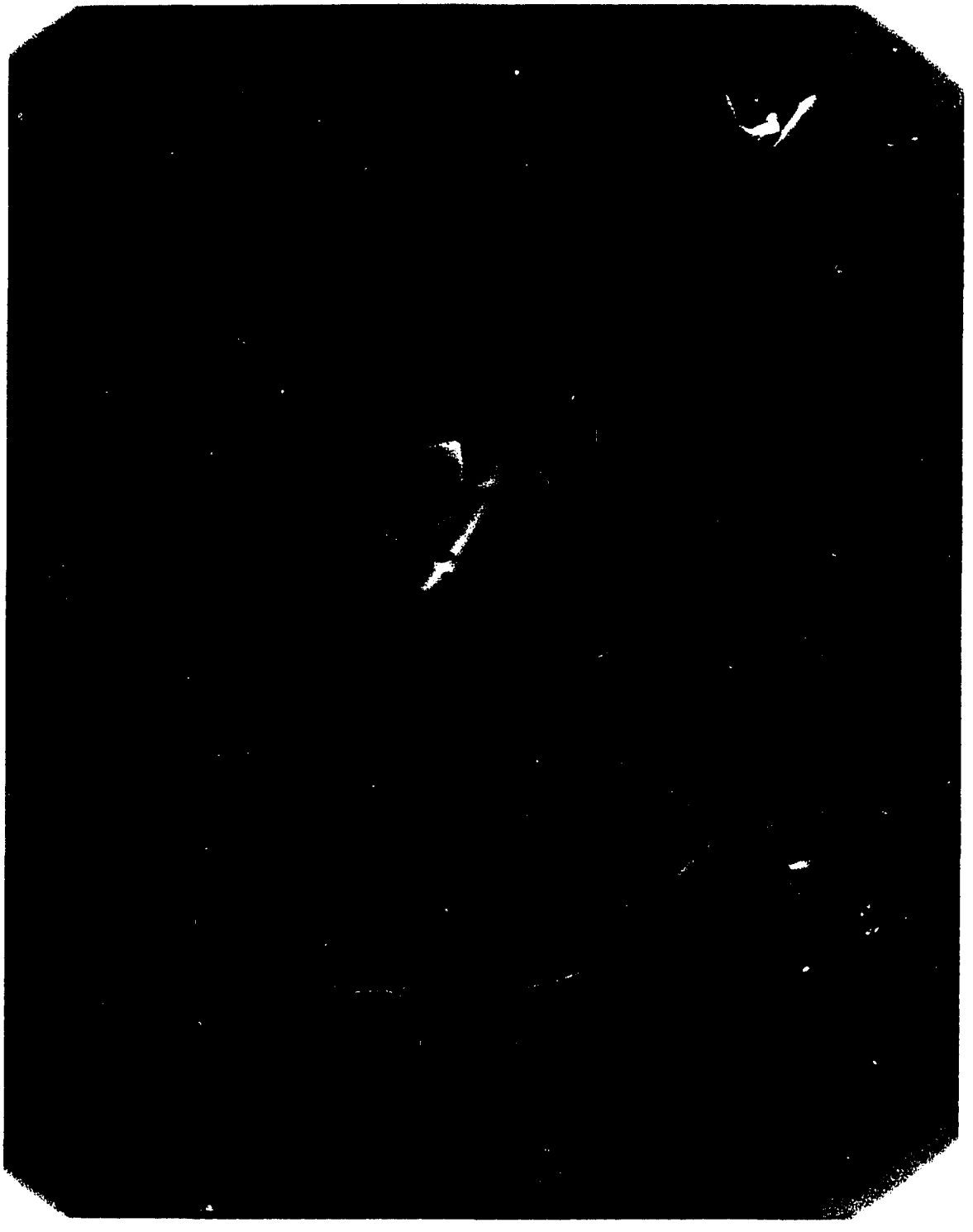

Figure 26. Magnification 1500X. Enlarged 1.6X. Numerical Aperature 1.4. Bright Field Illumination. High Purity Gold - Annealed. 100 Kev Protons. Blisters on Gold.

CHAPTER V

DISCUSSION OF RESULTS

Results obtained in this investigation make possible a reasonably consistent qualitative description of the proton irradiation induced blistering process in aluminum. The picture is by no means complete, nor are all of the mechanisms explained.

Although the aluminum oxide layer covering the metal lattice is considered to be relatively impervious to hydrogen (42-43), and any accumulation of hydrogen at the oxide interface would be expected to be temporarily trapped, it appears that the presence of the oxide is not a necessary prerequisite for blistering. Rather, the results suggest that blistering is a consequence of the lifting of the aluminum surface due to void formation within the aluminum lattice.

Since the protons introduced into the lattice are in solution at a concentration far in excess of the solubility of hydrogen in aluminum,* the protons would be expected to be rejected from the lattice in the form of hydrogen gas. The degradation of the lattice due to the proton irradiation (44-47) would be expected to produce regions of accumulated defects or voids which act as nuclei for bubbles(48). These

---

*Calculations based upon the assumption that the bombarding protons will come to rest in a region 0.1 to 0.5 micron thick show the hydrogen concentration to be from 1220 to 6100 ppm. for a total flux of 10^{17} p/cm^2.

bubbles would increase in size as the protons diffuse from the lattice into the voids. The process would cease only when the concentration of protons in the lattice was decreased to the solubility limit of hydrogen in aluminum at the temperature of concern. This hydrogen agglomeration just under the metal surface would cause localized swelling of the metal with consequent blister formation at the surface (Figures 27 and 28).

The principal contributions to the overall energy change associated with this blistering process are listed in equation 1:

$$\Delta F = -4/3\pi r^3 \Delta F_V + 4\pi r^2 S + 4/3\pi r^3 \Delta F_E \qquad \text{eq (1)}$$

where ΔF_V is the bulk free energy per unit volume associated with expulsion of the hydrogen from supersaturated solution in the metal lattice; S is the surface energy per unit area required for the formation of new surface, and ΔF_E is the lattice strain energy per unit volume required to produce the expansion of the voids. These terms comprise the net driving force for the formation of blisters, with ΔF_E and S the principal forces retarding the growth of voids and ΔF_V the driving force favoring the growth of voids.

Hydrogen agglomeration may be spontaneous, or it may require an elevated temperature anneal. "Spontaneous" blisters, i.e., blisters observed on samples not subjected to post-irradiation elevated temperature annealing treatments, were observed on aluminum irradiated with protons of 70 Kev energy or less upon initial microscopic examination approximately one week after irradiation. Optical and electron microscope examination of 100 Kev proton irradiated samples in the as-irradiated condition after two months storage at room temperature revealed a light distribution of blisters. Although no blistering was detected on 100 Kev

Figure 27. Annotated Illustration of Irradiation and Blistering Process.

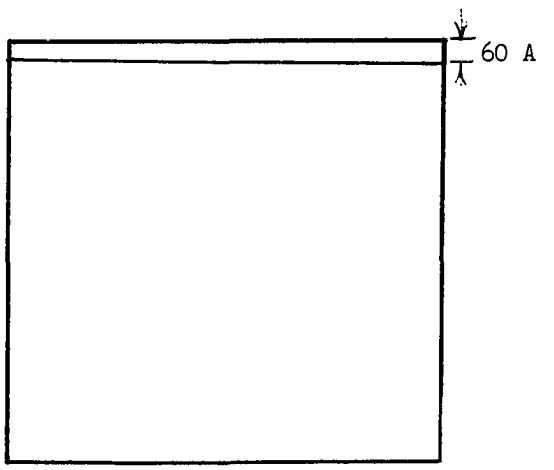

a. Sample before irradiation with an oxide layer of approximately 60 Å thick.

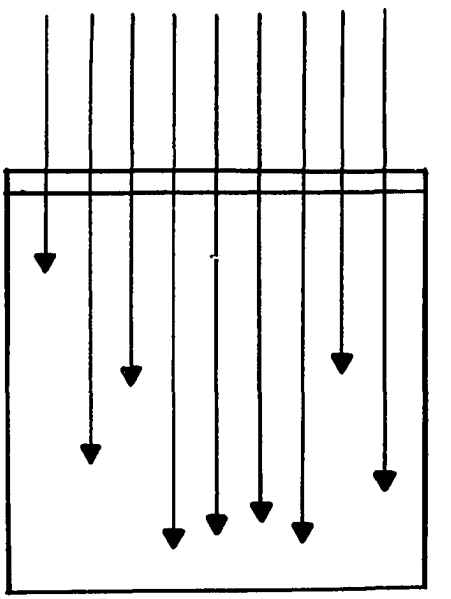

b. During 100 Kev irradiation the average proton penetration is 1/2 to 1 micron.

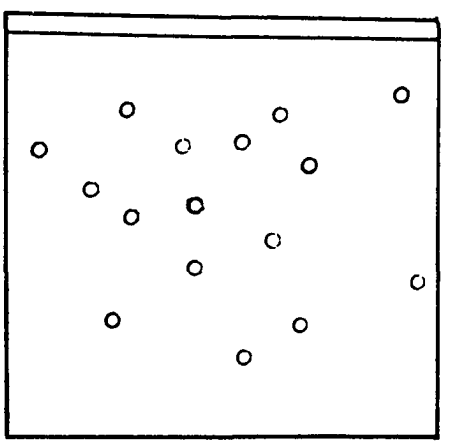

c. Initial agglomeration of protons to form hydrogen filled voids.

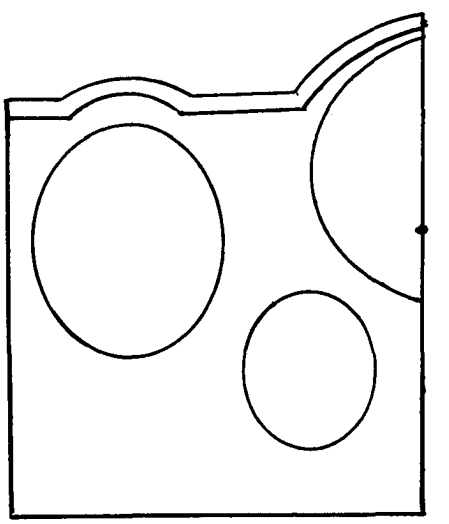

d. Upon annealing the small voids coalesce to form larger voids giving rise a surface blistering effect.

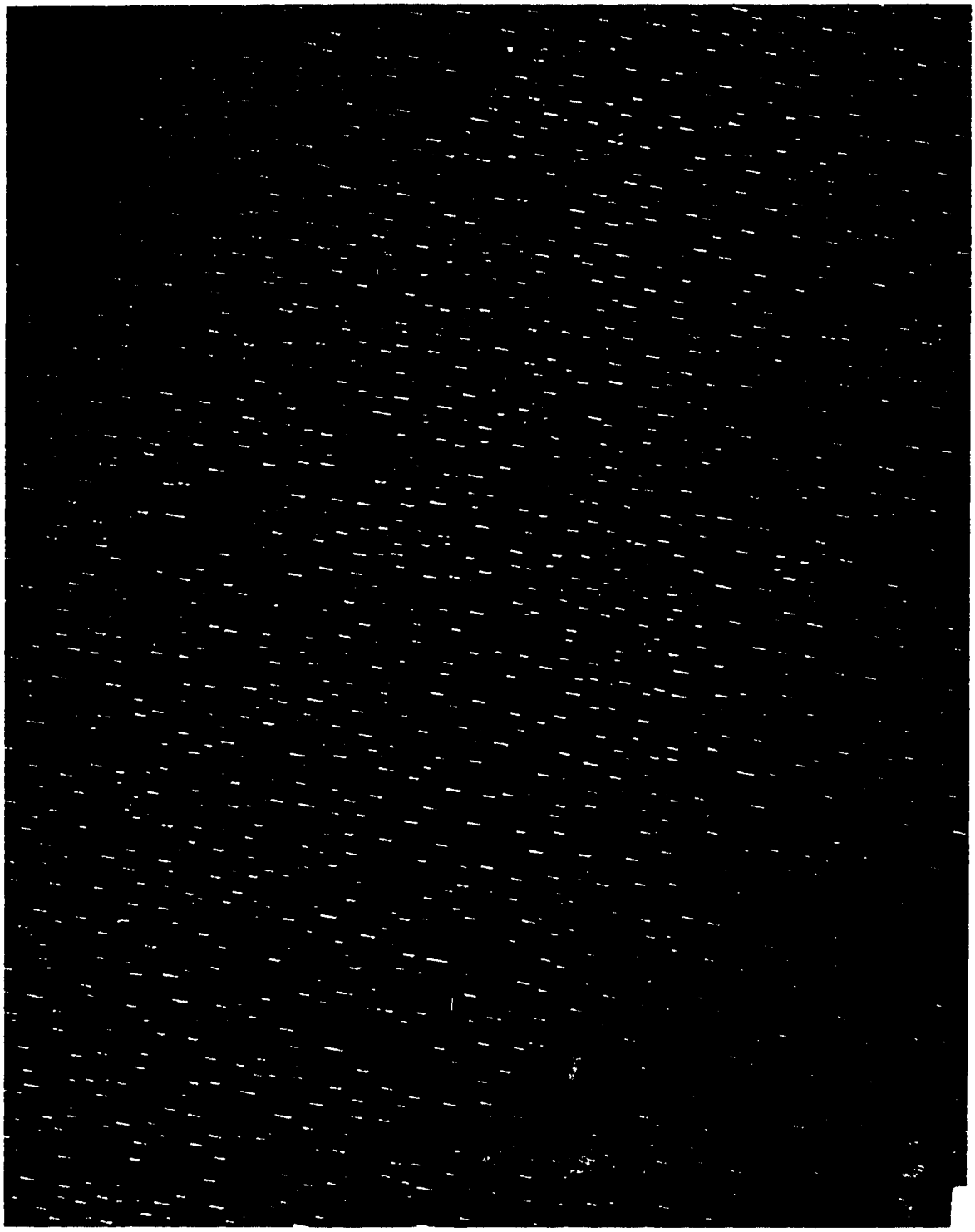

Figure 28. Magnification 1500X. Enlarged 1.6X. Numerical Aperature 1.4. Bright Field Illumination. High Purity Aluminum - Annealed with Oxide Chemically Removed. 100 Kev Protons.

proton irradiated specimens in the as-irradiated condition, this may not be considered as conclusive evidence that they did not exist, for only the optical microscope was used in this initial examination, and the presence of blistering at an early stage of development would have been undetected. A variation of spontaneous blister size with proton energy was noted. Lower energies produced blisters which were detectable with the optical microscope while higher energies produced spontaneous blisters of a smaller size which could be detected only with the electron microscope.

Aluminum specimens irradiated with protons of 100 Kev energy or higher and annealed at 300°C. produced fully developed blistering in approximately six minutes while annealing at 200°C. produced no blistering visible with the optical microscope even though the samples were allowed to remain at this temperature for durations up to 24 hours. Samples irradiated at energies greater than 70 Kev which were annealed soon after irradiation at temperatures of 250°C. or higher for sufficient periods of time exhibited a heavy concentration of blisters; samples which were allowed to remain in the as-irradiated condition for approximately 60 to 90 days to produce fine "spontaneous" blisters produced very little additional blistering upon annealing at temperatures above 200°C. Also, the samples which were annealed for long durations at 200°C. or less produced very light blister concentrations upon further annealing at temperatures of 250°C. or higher.

The development of spontaneous blisters on specimens irradiated at higher energies indicates some degree of hydrogen diffusion in aluminum at room temperature. Two experimental values of diffusivity of

hydrogen in aluminum are available in the literature:

$$D = 1.2 \times 10^{5} \exp(-33{,}500/RT) \quad (49)$$

and

$$D = 0.21 \exp(-10{,}900/RT) \quad (50)$$

Extrapolation to room temperature yields the values of 5×10^{-20} and 2×10^{-9} cm^2/sec, respectively, for D. Ells and Evans (11) concluded that only the values of D from the second equation would permit significant diffusion at lower temperatures. It is possible that the extrapolated value of D is in error, with the true value being larger, for the reported measurements in deriving these equations were made in the temperature range of 450-600°C. and cannot be expected to yield reliable values at temperatures as low as room temperature. Also, the material in the proton containing region, where the hydrogen diffusion is expected to occur, may not be considered to be in a fully annealed condition since some degree of structural damage has certainly been introduced by the bombarding ions. This damage may only be an introduction of point or line defects (44), or it may be complete polygonization with the formation of new grains within the original grains (45-47). This degradation of the existing lattice would be expected to increase the diffusivity over the reported value and, therefore, provide for the possibility of hydrogen agglomeration at room temperature.

The light concentration of blisters observed upon aluminum specimens irradiated at high energies, and which were either allowed to remain at room temperature for approximately 60 to 90 days or annealed at 200°C. for extended periods, suggests a second possible process for the rejection of hydrogen from the proton rich layer. This process must involve the general dispersion of hydrogen into the surrounding

hydrogen-free lattice. This again is a diffusion controlled process. These two mechanisms of hydrogen rejection (void formation and general dispersion) apparently compete for the available hydrogen. At low temperatures the conditions for general dispersion of hydrogen are apparently more favorable while at higher temperatures the void formation mechanism is the dominant means of removing the hydrogen from the lattice.

If the damage to the metal lattice produced by proton bombardment is assumed to provide sufficient and satisfactory nucleation sites (44-48), the kinetics of void formation in irradiated aluminum is apparently dependent upon the ability of the metal lattice to reject hydrogen to these nucleation sites. At low temperatures ΔF_v the driving force to reject the protons from the metal lattice into voids, thus producing pockets of hydrogen, is apparently unable to overcome the resistance to void expansion associated with ΔF_E the strain energy in the metal lattice. This is the case where the depth of proton penetration is greater. In specimens irradiated at lower energies where the proton penetration is less, the resistance to void expansion is lower because of the proximity of the void to a free surface. The correspondingly lesser penetration associated with lower energy protons produces voids with a much thinner layer of metal on the free surface side of the void, which effectively lowers the value for ΔF_E and permits expansion of the void in the direction of this free surface with relatively low gas pressures within the void. The greater depth of penetration associated with the higher proton energies produces voids deeper within the metal requiring higher gas pressures to cause an expansion of the void and consequent swelling or blistering of the metal surface.

The variation in the thickness of the blister wall expected with proton energy appears to be substantiated by observations on sample surfaces. Figure 29 illustrates a 50 Kev proton irradiated specimen surface upon which some collapsed blisters can be seen. Blisters caused by higher energy protons with a correspondingly thicker layer of metal on the free surface side of the void do not collapse, Figures 30 and 31.

At high temperatures the metal lattice is weaker allowing the driving force for rejection of hydrogen from the metal lattice ΔF_V to overcome the resistance to void expansion associated with the volume strain energy ΔF_E. In specimens irradiated at higher energies and annealed at high temperatures, the void formation mechanism is apparently capable of competing for the available hydrogen with the general dispersion mechanism, and, therefore, voids with the resulting blisters are formed. At low temperatures the metal lattice is stronger; the driving force to reject the hydrogen from solution, ΔF_V, is unable to overcome the resistance to void expansion, ΔF_E, and only a limited number of nucleated sites can grow to sufficient size to produce blisters on the surface of higher energy irradiated specimens.

Two forms of oxide removal appear to occur on aluminum surfaces subjected to proton bombardment. The optical microscope revealed a pitting of the oxide, and the electron microscope revealed an additional more general removal of surface material. While the latter more general removal of surface material is expected and is attributed to the normal sputtering process, the localized pitting is not as readily explained. Although the existence of localized variations in the characteristics of the oxide due to impurities or defects in the substrate aluminum cannot



Figure 29. Magnification 11,000X. Electron Micrograph. High Purity Aluminum-Annealed with Oxide Chemically Removed. 50 Kev Protons. Elongated Blisters Some of which have Collapsed.



Figure 30. Magnification 11,000X. Electron Micrograph. High Purity Aluminum-Annealed. 100 Kev Protons. Pitting and Blistering with Concentration Variation Between Two Grains.



Figure 31. Magnification 9,500X. Electron micrograph. High Purity Aluminum-Annealed with Oxide Chemically Stripped. 100 Kev Protons. Blisters at Edge of Irradiated Area. Irradiated Area is at Upper Right.

be discounted as a cause for localized pitting, a second mechanism based upon blister formation at the oxide-metal interface is possible. The large amount of surface oxide removal on some samples irradiated in the 30-50 Kev energy range (Figures 9-10) supports the concept that blisters which form at the oxide-metal interface cause an exfoliation of the oxide. Formation of such blisters at the base of the oxide may also have been the cause of pitting observed at other energies. Credence is given to this mechanism by the observation that blistering was not readily observed with the optical microscope at energies below the energy range associated with complete oxide removal. This indicates that the mean penetration range of the protons at 30-50 Kev is approximately equal to the oxide thickness, and as the proton energy is varied above or below the 30-50 Kev energy level, the penetration is greater than or less than the oxide thickness. Figure 32 is an electron photomicrograph of an as-irradiated specimen on which the oxide is lifted from the underlying metal to form blisters. Some of the blisters have their tops removed and appear to be in an early stage of exfoliation. After stripping the oxide there was no evidence of blistering or pitting on this sample indicating that these effects were confined to the oxide layer. Subsequent annealing produced normal blistering associated with void formation within the metal lattice.

Specific observations of pitting and blistering were greatly influenced by the purity, defect structure, and orientation of the material. Study of the effects of impurities was limited to observations of a greater concentration of blisters occurring along the boundaries of what were suspected to be impurity-rich regions in remelted aluminum.

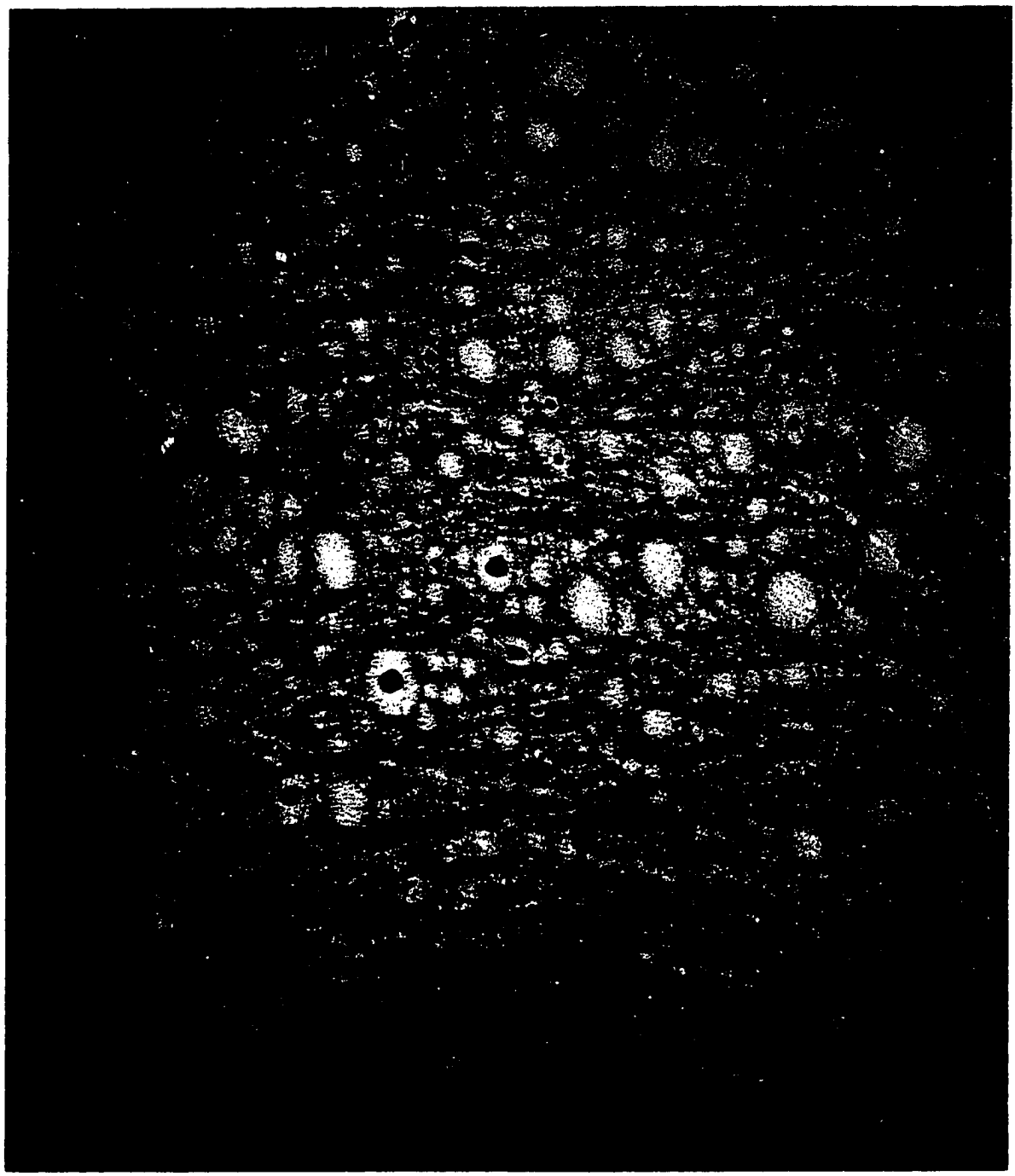

Figure 32. Magnification 11,000X. Electron Micrograph. High Purity Aluminum-As-Irradiated. 100 Kev Protons. Blistering Due to Void Formation at Oxide-Metal Interface. Note the Removal of Oxide from the Surfaces of Some Voids.

This impurity structure is associated with a segregation of impurities to selective regions of the material during solidification. The phenomenon of a cellular or lamaller substructure extending parallel to the crystal growth direction has been observed for conditions of unidirectional solidification of crystals from the melt (51).

A recent study of such impurity segregation in aluminum by electron microprobe analysis demonstrates that the impurity concentration necessary for the substructure formation is well within the impurity level of 99.997^{+} aluminum (52). The study further indicated that the concentration enhancements in the region of microsegregation can be as much as two orders of magnitude with iron being the primary segregating impurity in the material studied.

It is reasoned that the agglomeration of protons to form hydrogen pockets occurs more readily in the presence of impurities, either because of a lowered surface energy or because a greater concentration of defects in the impurity containing regions may provide paths for rapid diffusion of hydrogen, or both. The result would be a higher than normal concentration of blisters in these regions of the sample. The presence of these impurities distorts the perfection of the metal lattice, thus reducing the ion penetration depth (53), and, thereby, effects the blister concentration in these regions. A more specific delineation of the effects of impurities upon the observed processes is difficult since information in the literature concerning such factors as the solubility of hydrogen in aluminum and the thickness variation of the surface oxide film versus impurities are somewhat conflicting and limited (31).

While the specific effects of impurities and cold work upon the tendency to form blisters were difficult to differentiate in the alloy specimens, the effects of cold work in the high purity aluminum are readily evident in Figure 24. The large blisters situated along the scratches on the metal surface suggest that cold working of the material has introduced paths of high hydrogen diffusivity in the deformed metal lattice. Apparently the hydrogen is able to move relatively long distances along the paths to form fewer voids which are of much greater size than seen in non cold worked regions.

The correlations of the occurrence of pitting and blistering with orientation, illustrated in Figures 6 and 8, indicate a combined dependence of pitting and blistering upon orientation. Since any surface pitting effects attributed to particle radiation are due to a high degree of interaction of the bombarding ions with the surface material, the heavy pitting of the aluminum oxide indicates that the ion penetration depth is less or the ion interaction is greater in such regions than in those regions where a relatively low pitting concentration occurs. Also, the observation of spontaneous blisters upon specimens irradiated at 10-30 Kev suggests that the lack of blistering upon some grains of specimens irradiated at higher energies may be due to the protons being situated at such depths that most voids which form would not cause a swelling of the metal surface. Therefore, possible explanations of the blister and pit concentration dependence on orientation may involve variations in ion penetration depth or in ion interaction with the surface atoms.

Piercy and collaborators (27) have reported a channeling or greater depth of penetration of heavy ions in aluminum along specific crystallographic directions. This orientation dependence of the range is a consequence of the tendency of the lattice to focus moving particles along channels bordered by relatively closely packed atomic rows (26). Channeling has been reported along the most open directions of the face centered cubic lattice with the greatest degree of penetration occurring along the [110] direction followed by the [100] and [111] directions.

Channeling of bombarding ions into the lattice and sputtering or ion interaction with surface atoms appear to be related effects with each depending upon the ability of the lattice to stop impinging ions. The (111) plane, being the most closely packed plane and associated with the least open direction, allows the least transparency to bombarding ions, and consequently the [111] direction has the highest sputtering yield followed by the [100] and [110] directions (54-56). This behavior is reported to vary only in the low energy region ($<$1 Kev) where a reversal occurs and the sputtering yield of the (100) plane becomes greater than the (111) plane (57). These observations suggest that at the very low energies the stopping power of the metal lattice is no longer the controlling parameter, and the bonding energy of the metal surface atoms dominates the low energy sputtering process.

Results of research in the fields of channeling and sputtering appear to be consistent in that the more open lattice directions show a greater ion penetration depth and a lower sputtering yield. This information from the literature is not in accord with the results presented here which would lead one to believe, if the suggested mechanism is

appropriate, that the penetration depths are greatest along the [111] direction followed by the [100] and [110] directions, with sputtering yields in the reverse order of penetration depths.

The lack of correlation of observations of the orientation dependence of pitting and blistering reported in this work with the crystal orientation dependent lattice damage and penetration depths reported in the literature appears to discredit any dependence of the pit and blister concentrations upon the channeling of ions or sputtering. This lack of correlation may be due to the use of very small and light hydrogen ions in this work; whereas the results reported in the literature are for larger and heavier bombarding ions. However, this variation in technique appears inadequate to explain the lack of correlation when account is taken of the fact that the [111] direction in fcc lattice which shows the lowest pit and blister concentrations is not an open direction.

An alternate approach to an explanation of the orientation dependence of pitting and blistering is to consider the reaction of the ion within the metal lattice after having come to rest. This approach is one of considering the effects of crystal orientation upon the behavior of hydrogen in the metal.

The mechanisms proposed for pitting and blistering require the hydrogen to be deposited at shallow depths or to be capable of migration to shallow depths. This migration requires transport of hydrogen, and variation of pit and blister concentrations with orientation may be a variation of this transport process with crystal orientation. Although there is general agreement in the literature that certain crystallographic

directions should offer easier paths for interstitial diffusion through a metal lattice (58), there is little experimental evidence in the literature to confirm this. Transport could also occur preferentially along paths introduced into the lattice by the ion irradiation. These paths could be accumulations of defects which possess an orientation dependence. How these defect enhanced diffusion paths could be related to crystallographic orientation is not known.

The hydrogen atom may occupy either of two types of interstitial sites available in the fcc lattice. The larger of these two types of sites is formed by six metal atoms in an octahedral formation and has a radius of 0.414 R where R is the radius of the fcc lattice atoms. The smaller site is formed by four metal atoms in a tetrahedral formation and has a radius of 0.28 R. The available information in the literature is not conclusive as to which of these two sites is favored as a residence for a hydrogen ion although there appears to be a preference in the more recent literature for choosing the octahedral site. The fcc unit cell composed of 12 metal atoms (4 equivalents) also contains 12 octahedral interstitial sites. An octahedral site has 12 nearest neighbor octahedral sties which lie equidistant along $\langle 110 \rangle$ directions from the site of concern.

An analysis of the possible transport of interstitial atoms in the [100], [110], and [111] directions by diffusion considering only the octahedral sites is readily accomplished since the jump frequency of the interstitial to any one of its 12 nearest neighbor sites is uniform. Such an analysis reveals no variation of diffusion rates in these three low index directions. An analysis of the diffusion process utilizing

the octahedral sites and the smaller tetrahedral sites is not feasible because the jump frequencies of the interstitial among the two different sized interstitial sites is not known.

Although no direct evidence can be found to substantiate the possibility of orientation dependent diffusion rates, such variations appear to be involved in the blistering and pitting process. The diffusion rates appear to increase as the crystallographic directions proceed from the most closely packed planes to the most open directions. The highest diffusion rate results in the [110] direction while the lowest diffusion rate occurs in the [111] direction which presents the most closely packed surface.

CHAPTER VI

CONCLUSIONS

1. Pitting and blistering of high purity gold and aluminum produced by low energy proton bombardment have been studied. This research was conducted to determine and study the mechanisms of the pitting and blistering processes and the environmental parameters which affect these processes.

2. Pitting and blistering of high purity aluminum occurs on the surface of aluminum specimens subjected to proton bombardment in the energy range 7 to 450 Kev to a total flux of 10^{16} p/cm^2 or greater. The pitting occurs upon irradiation while the formation of blistering requires either time or elevated temperature or both.

3. Pitting is the result of accumulation of protons as hydrogen in voids which form at the oxide-metal interface. Pitting was observed on aluminum at all proton bombardment energies studied. Irradiation at a low temperature (-200°C.) or a high temperature (+200°C.) tended to suppress the formation of pitting.

4. Blistering occurs spontaneously at room temperatures on samples irradiated at energies of 70 Kev or lower. Samples irradiated at energies of 100 Kev or higher show a lesser amount of spontaneous blister formation at room temperature, and an elevated temperature

anneal is required to produce fully developed blisters. Blisters appear to be the result of agglomeration of hydrogen into relatively shallow voids within the metal matrix where the presence of the free surface allows an outward expansion.

5. The blisters observed on samples which were irradiated at the lower proton energies formed spontaneously. This behavior is attributed to shallower penetration depths of the lower energy protons which permit expansion of voids at lower hydrogen pressures. For the greater proton penetration depths associated with higher energy irradiation, annealing is required to produce blistering because of the greater diffusion distance and the higher gas pressures necessary to cause expansion of the voids.

6. The concentration and size of blisters on aluminum, obtained on annealing, were a function of the annealing temperature. Annealing of higher energy irradiated aluminum at temperatures of 250°C. or higher produced a heavy concentration of blisters while annealing at 200°C. produced no blisters. The higher annealing temperature favored agglomeration of hydrogen into voids while the lower temperature favored a general dispersion of hydrogen throughout the lattice.

7. Gold samples were irradiated with 100 Kev and 50 Kev protons. No pitting or blistering were observed on samples irradiated at 50 Kev. Samples irradiated at 100 Kev blistered after annealing at 300°C. It is concluded from the presence of blisters on gold in the absence of an oxide layer that the presence of an oxide is not a prerequisite for blistering. The absence of pitting on gold further supports the conclusion that the pitting is caused by trapping of protons under the oxide.

8. The size and distribution of pits and blisters were demonstrated to be sensitive to metal purity and microstructure. The presence of impurities increases the size of the blisters and increases the concentration of blisters. The agglomeration of protons to form hydrogen pockets occurs more readily in the presence of impurities, either because of a lowered surface energy or because a greater concentration of defects in the impurity containing regions may provide paths for rapid diffusion of hydrogen. Both factors may contribute to the observed effects.

9. The presence of cold work in the material produces an increase in the size of the blisters. The increase in blister size suggests that the cold working of the material has introduced paths of high hydrogen diffusivity in the deformed metal lattice.

10. A dependence of pit and blister concentration on crystal orientation indicates that the processes responsible for the formation of pits and blisters are dependent on lattice atom arrangements. This dependence may arise as the protons enter and pass through the lattice, or it may occur when the protons as hydrogen atoms try to leave the proton rich regions by a lattice diffusion process. Since the effects of orientation upon pitting and blistering are not in agreement with the results of studies on energetic ion channeling and sputtering cited in the literature, it is concluded that the transport rate of hydrogen must vary with crystal orientation. This variation of transport rate may be characteristic of a perfect fcc lattice, or it may be movement along orientation dependent imperfections introduced into the lattice by the proton irradiation.

APPENDIX A

DETERMINATION OF NATURAL OXIDE FILM THICKNESSES ON ALUMINUM

The technique used for the determination of the natural oxide film thickness was developed by M. S. Hunter, P. Fowle, and P. F. Towner (Alcoa Research Laboratories) (59,60). It is based on a combination of the characteristics of barrier layer type anodic coatings and interference color methods.

Natural oxide films on aluminum consist of two layers, a barrier layer (the inner layer), and a porous layer (the outer layer). The electrical properties of the porous layer are such that it offers little resistance to current flow. The barrier layer, however, acts as a dielectric, and its properties are such that when an anodizing process is carried out in the proper type of electrolyte, the thickness of the barrier layer will be increased by 14 Å/volt while the thickness of the porous layer will remain constant. The basic requirement of the electrolyte is that it must not exert a solvent action on the oxide. A 3% solution of ammonium tartrate adjusted to a pH of 5.5 is commonly used.

Using the 14 Å/volt relationship for barrier layer type oxide, the thickness of the natural barrier layer can be determined. If the thickness of the natural barrier layer is t angstroms, for any applied

voltage less than t/14 the thickness of the natural barrier layer will not be affected. However, for a voltage of t/14 plus some small increment, a small amount of barrier layer oxide will be formed. This formation will be accompanied by a significant rise in current flow above that of the natural leakage flow. Therefore, the process for determining the natural barrier layer thickness is to increase the voltage in small increments until a significant current rise (which will be followed by a current drop after the oxide has been formed) is observed. The applied voltage multiplied by the 14 Å/volt constant will give the thickness of the natural barrier layer.

The thickness of the porous layer is determined from interference colors. Natural oxide is not thick enough to give interference colors. However, the thickness of the oxide can be increased to any desired amount by anodizing. When the thickness is increased to give the desired interference colors (the blue-green range for 4th order interference has proved to be most desirable to detect changes in colors for small changes in film thickness), the thickness of the barrier layer oxide is known from the 14 Å/volt relationship. For example, if a sample is anodized to 200V, the total thickness of barrier layer oxide (the natural barrier layer plus the amount that is added) will be 2800 Å. In the anodizing process the thickness of the porous layer remains unchanged. Therefore, the total thickness of the oxide minus the thickness of the barrier layer oxide will give the thickness of the original porous layer of the natural oxide.

The total thickness of the oxide on an unknown sample after anodizing is determined by matching its interference colors with those

of a standard sample whose thickness is known. The standard sample is prepared by stripping its oxide in a chromic acid - phosphoric acid solution. This solution will remove the oxide but will not attack the aluminum. The standard is then anodized to some voltage slightly above that to which the unknown sample was anodized. Since all the oxide is stripped from the standard before anodizing, the oxide on the standard after anodizing consists only of barrier layer oxide, and its thickness can be calculated from the anodizing voltage and the 14 Å/volt constant.

It was stated above that the standard sample is prepared by anodizing to some voltage slightly above the voltage to which the unknown sample is anodized. The interference colors from the two samples are then compared. If they do not match, the standard sample is anodized to a slightly higher voltage, and the comparison is made again. This process is continued until the colors from the two samples match. When the colors match, this means that the total oxide thicknesses of the two samples are equal. The total oxide thickness of the standard sample is known from its anodizing voltage, and the barrier layer oxide thickness of the unknown sample is known from its anodizing voltage. Therefore, the thickness of the porous layer oxide on the unknown sample is the difference between these two known thicknesses.

Best results in the color matching process can be obtained by preparing two standard samples and keeping a one volt difference in their anodizing voltages. Differences in interference colors for a one volt difference in anodizing voltage can be detected quite readily. Therefore, if the oxide thicknesses of the two standards are adjusted (keeping a one volt difference in their anodizing voltages) until the

color of the unknown sample falls between the colors of the two standards, the porous oxide thickness can be determined to at least ± 0.5 volts, or ± 7 Å. This accuracy can be increased with the experience of the operator. An experienced operator should have no trouble detecting color changes for a 1/2 volt difference in anodizing voltages.

APPENDIX B

Two limiting cases of hydrogen containing void formation within the metal lattice can be considered. One is the formation of a void at a depth where the effects of the free surface are not a factor. The other is the formation of a void at a relatively shallow depth where the expansion of free surface to form blisters is the controlling process. The pressure inside a void which is not affected by the free surface is given by the equation:

$$P_{H_2} = \frac{2\sigma}{r} \qquad \text{eq. (1)}$$

where P_{H_2} is the pressure of hydrogen in the void

σ is the surface tension

r is the radius of the bubble.

The pressure inside a void which is near a free surface can be approximated by use of an equation for the critical pressure to cause the onset of buckling of a circular plate which is clamped at its edges. This equation (61) is:

$$P_{cr} = \frac{4\sigma_y \ t_p^2}{3r_p^2} \qquad \text{eq. (2)}$$

where σ_y is the yield strength of the material

t_p is the thickness of the plate, corresponding to the wall thickness of the blister or distance from the free surface

r_p is the radius of the plate, corresponding to the radius of the blister.

As voids are initiated for each of these two limiting cases the pressure requirement to cause initial growth is given by equation 1, but as growth proceeds the void nearer the surface will be influenced by the free surface. As the pressure increases this shallow void will experience an expansion in the direction of the free surface with formation of a blister. This process is approximated by equation 2 where it is assumed the thin wall on the free surface side of the void may be considered analogous to a circular plate which is clamped at its edges and subjected to a pressure on one surface. Using a value of 120,000 grams/cm^2 for σ_y, 0.1 micron for t_p, and 0.5 micron for r_p, equation 2 yields a critical pressure for buckling of 4.1×10^6 dynes/cm^2. Assuming a value of 1000 dynes/cm for and 0.5 micron for r, equation 1 yields a pressure of 410×10^6 dynes/cm^2 for a similar size void deep within the material.

Under the conditions assumed above there is an appreciably lower pressure requirement for void growth near the free surface than for voids deeper within the metal. It is obvious from examination of equations 1 and 2 that this difference in pressure is rapidly diminished as voids of smaller radius are considered. This behavior substantiates the statement that when the voids are small they behave in the manner predicted by equation 1. Equation 2 is valid only when the thickness of the plate is much smaller than the radius of the plate.

Consideration of the effects of temperature upon the two limiting cases for void formation reveals that changes in the diffusion rate will

have a common effect upon both situations. The increase in the diffusion rate associated with higher temperatures produces a faster expulsion of hydrogen from the surrounding lattice and into the voids. This increased diffusion rate also replenishes the depleted region surrounding the void allowing further growth of the void. The increase of temperature will also increase the pressure of a constant number of moles of gas contained within an existing void. This pressure increase will promote the buckling of the thin circular plate covering the shallow void. However, the pressure increase in the deeper void will tend to drive the hydrogen back into solution since there is no free surface to relieve this pressure increase.

LIST OF REFERENCES

1. Andrews, A., et al. "Penetrating Radiation," Space Materials Handbook. Addison-Wesley Publishing Co., Reading, Massachusetts. 1965. pp. 51-76.

2. Wehner, G. K. "Sputtering by Ion Bombardment," Advances in Electronics and Electron Physics. Vol. 7. Academic Press, Inc., New York. 1955. pp. 239-97.

3. Anderson, D. L., and Dahms, R. G. "Surface Blistering of Metals Due to Low Energy Hydrogen Ion Bombardment," American Institute of Aeronautics and Astronautics, and American Society of Mechanical Engineers, Structures and Materials Conference. American Institute of Aeronautics and Astronautics, New York. 1966. pp. 216-223.

4. Gillette, R. B., Brown, R. R., Seiler, R. F., Sheldon, W. R. Space Radiation Tests on Reflecting Surfaces. Final Report JPL Lab. Contract No. 950998, June, 1965.

5. Wilkinson, W. D., and Murphy, W. F. Nuclear Reactor Metallurgy. D. Van Nostrand Co., Inc., Princeton, N. J. 1958.

6. Barnes, R. S., and Mazey, D. J. "The Migration and Coalescence of Inert Gas Bubbles in Metals." Proc. Roy. Soc. (London) Ser. A 275: 47-57. 1963.

7. Shewman, P. G. "The Movement of Small Inclusions in Solids by a Temperature Gradient." Trans. Met. Soc. of AIME. 230: 1134-37. 1964.

8. Barns, R. S. "A Theory of Swelling and Gas Release for Reactor Materials." J. Nucl. Mat. 11: 135-48. 1964.

9. Greenwood, G. W. "Role of Fission Gas Re-solution During Post Irradiation Heat Treatment." J. Nucl. Mat. 3: 234-40. 1962.

10. Boltax, A. "Metallographic Study of Swelling in Alpha-particle Irradiated Al and Al Alloys." J. Nucl. Mat. 7: 1-15. 1962.

11. Ells, C. E., and Evans, W. "The Agglomeration of Hydrogen in Aluminum." Trans. AIME. 227: 437-46. 1963.

12. Kaminsky, M. "Mass Spectrometric Studies of the Species of Particles Leaving a Monocrystalline Target in a Charged or Uncharged State Under High Energy Ion Bombardment." Adv. in Mass. Spec. 3: 69-90. 1964.

13. Pemsler, J. P. and Rapperport, E. J. "Hydrogen in Proton Bombarded Beryllium Agglomeration and Diffusion." Trans. AIME. 230: 90-94. 1964.

14. Gillette, R. B., Brown, R. R., Seiler, R. F., Sheldon, W. R. Effects of Proton and Alpha Particles on Thermal Properties of Spacecraft and Solar Concentrator Coatings. AIAA Thermophysics Specialist Conference, Monterrey,Calif., Sept. 13-15, 1965.

15. Primak, W., and Luthra, J. "Radiation Blistering: Interferometric and Microscopic Observations of Oxides, Silicon, and Metals." J. Appl. Phys. 37: 2287-2294. 1966.

16. Cunningham, R. L., Haymann, P., Moore, W. J., and Trillat, J. J. "Etching of Surfaces with 8 Kev Argon Ions." J. Appl. Phys. 31: 839-842. 1960.

17. Kueck, P. D., and Brewer, A. K. "Aluminum Sputtering by Helium." Rev. Sci. Instr. 3: 427-429. 1932.

18. Wehner, G. K., Rosenberg, D. L., and KenKnight, C. E. Investigation of Sputtering Effects on the Moon's Surface. NASA Contract NASw-751 Reports.

19. KenKnight, C. E., and Wehner, G. K. "Sputtering of Metals by Hydrogen Ions." J. Appl. Phys. 35: 322-26. 1964.

20. Wehner, G. K., Rosenberg, D. L., and KenKnight, C. "Sputtering Rates Under Solar Wind Bombardment." Planetary and Space Sci. 11: 885-95. 1963.

21. Wehner, G. K., KenKnight, C. E., and Rosenberg, D. "Modification of the Lunar Surface by the Solar Wind Bombardment." Planetary and Space Sci. 11: 1257-61. 1963.

22. Young, J. R. "Penetration of Electrons and Ions in Aluminum." J. Appl. Phys. 27: 1-4. 1956.

23. Warshaw, S. D. "The Stopping Power for Protons in Several Metals." Phys. Rev. 76: 1759-65. 1949.

24. Wilcox, H. A. "Experimental Determination of Rate of Energy Loss for Slow H^1, H^2, He^4, Li^6 Nuclei in Au and Al." Phys. Rev. 74: 1743-54. 1948.

25. Van Wijngaarden, A., and Duckworth, H. E. "Energy Loss in Condensed Matter of H^1 and He^4 in the Energy Range 4 E 30 Kev." Can J. Phys. 40: 1749-1976. 1962.

26. Robinson, M. T., and Oen, O. S. "Computer Studies of the Slowing Down of Energetic Atoms in Crystals." Phy. Rev. 132: 2385-2398. 1963.

27. Piercy, G. R., McCargo, M., Brown, F., and Davies, J. A. "Experimental Evidence for the Channeling of Heavy Ions in Monocrystalline Aluminum." Can. J. Phys. 42: 1116-34. 1964.

28. Ransley, C. E., and Neufeld, H. "The Solubility of Hydrogen in Liquid and Solid Aluminum." J. Inst. of Met. 74: 599-620. 1948.

29. Kostron, H. "Aluminum and Gas." Zeitschrift für Metallkinde. 43: 269-284. 1952.

30. Opie, W., and Grant, N. "Effects of Hydrogen on Mechanical Properties of Some Aluminum Alloys." Foundry. 78: 104-109. 1950.

31. Sokolskaya, L. I. Gases in Light Metals. Pergamon Press, New York. 1961.

32. Toole, F. J., and Johnson, F. M. G. "The Solubility of Oxygen in Gold and in Certain Silver-Gold Alloys." J. Phys. Chm. 37: 331-346. 1933.

33. Davies, W. "The Rate of Heating of Wires by Surface Combustion." Phil. Mag. 17: 233-251. 1934.

34. Eichenauer. W., and Liebscher, D. "Determination of the Diffusion Speed of Hydrogen in Gold." Z. Naturforschg. 17a: 355. 1962.

35. Tegart, W. J. McG. The Electrolytic and Chemical Polishing of Metals. Pergamon Press, New York. 1959.

36. Lewis, J. E., and Plumb, R. C. "A Radiochemical Technique for Determining the Specific Surface Area of Aluminum Metal Surfaces." Inter. J. Appl. Radiation and Isotopes. 1: 33-45. 1956.

37. Lacombe, P., and Beaujard, L. "The Application of Etchfigures on Pure Aluminum (99.99%) to the Study of Some Micrographic Problems." J. Inst. Metals. 74: 1-16. 1948.

38. Rovinskii, B. M., Kostyukova, E. P., and Lyuttsau, V. G. "Substructure and Distribution of Dislocations in Single Crystal and Polycrystalline Al." Sov. Phy. Cryst. 8: 524-27. 1964.

39. Wyon, G., Marchin, J. M., and Lacombe, P. Les Memoires Scientifiques De La Revue de Metallurgie. 56: 1959.

40. Welsh, N. C. "Pseudo-subgrain Structures on Al Surfaces." J. Inst. Met. 85: 129-135. 1956-57.

41. Cuff, F. B., and Grant, N. J. "A Segregation Substructure in Aluminum. J. Inst. Met. 87: 248-54. 1958-59.

42. Smithells, C., and Ransley, C. "The Diffusion of Gases Through Metals (Diffusion of Hydrogen Through Aluminum)." Pro. Royal Soc. 152A: 706-713. 1935.

43. Russell, A. S. "Diffusion of Hydrogen Through Aluminum Tubes." Metal Progress. 55: 827-831. 1949.

44. Bowden, P., and Brandon, D. B. "Production of Interstitial Point Defects by Low Energy Ion Bombardments." J. Nucl. Mat. 9: 348-54. 1963.

45. Trillat, J. J. "Etude des Structures Superficielles par Diffraction Electronique que et Bombardment Ionique Combines, Applications." J. Chem. Physique. 33: 570. 1956.

46. Ogilvie, G. J., and Ridge, H. J. "The Cathodic Sputtering of Silver." J. Physik. Chem Solids. 10: 217. 1959.

47. Fansworth, H. E., Schlier, R. E., George, T. H., and Burger, R. M. "Ion Bombardment Cleaning of Germanium and Titanium and Determined by Low-Energy Electron Diffraction." J. Appl. Phys. 26: 252-253. 1955.

48. Greenwood, G. W., Foreman, A. J. E., and Rimmer, D. E. "Role of Vacancies and Dislocations in the Nucleation and Growth of Gas Bubbles in Irradiated Fissile Material." J. Nucl. Met. 4: 305-24. 1959.

49. Ransley, C. E., and Talbot, D. E. J. "Wassenstoff Porositaet in Metallen." Zeitschrift für Metallkinde. 46: 328-37. 1955.

50. Eichenauer, W., and Pebler, A. "Wasserstoff in Aluminum and Kupfer." Zeitschrift für Metallkunde. 48: 373-78. 1957.

51. Chalmers, B., and Rutter, J. W. "Prismatic Substructure Formed During Solidification of Metals." Can. J. Phys. 31: 15-39. 1953.

52. Biloni, H., Bolling, G. F., and Domain, H. A. "Electron Microprobe Analyses of Segregation Produced During Cellular Solidification of "Pure" Aluminum." Trans. Met. Soc. AIME. 233: 1926-32. 1965.

53. Farmery, B. W., Nelson, R. S., Sizmann, R., Thompson, M. W. The Channelling of 2.5 Mev Protons in Cu and Some Effects of Temperature and Radiation Damage. United Kingdom Atomic Energy Authority. AERE-R5089. 1965.

54. Magnuson, G. D., and Carlston, C. E. "Sputtering Yields of Single Crystals Bombarded by 1 to 10 Kev Ar^+ Ions." J. Appl. Phys. 34: 3267-3273. 1963.

55. Southern, A. L., Willis, W. R., and Robinson, M. T. "Sputtering Experiments with 1 to 5 Kev Ar^+ Ions." J. Appl. Phys. 34: 153. 1963.

56. Rol, P. K., Fluit, J. M., and Kisternmaker, J. "Sputtering of Copper by Bombardment with Ions at 5-25 Kev." Physica. 26: 1001-1011. 1960.

57. Zdanuk, E. J., and Wolsky, S. P. "Sputtering of Single Crystal Cu and Al with 20-600 ev Ar^+." J. Appl. Phys. 36: 1683-87. 1965.

58. Smialowski, M. Hydrogen in Steel. Pergamon Press, New York, 1962.

59. Hunter, M. S., and Fowle, P. "Determination of Barrier Layer Thickness of Anodic Oxide Coatings." Journ. of the Electrochemical Soc. 101: 481-485. 1954.

60. Hunter, M. S., and Towner, P. F. "Determination of the Thickness of Thin Porous Oxide Films on Al." Journ. of the Electrochemical Soc. 108: 139-144. 1961.

61. Faupel, J. H. Engineering Design. John Wiley and Sons, Inc., New York. 1964.